Soft Gripper Driven by a Solenoid Actuator

by

Sepehr Sheikholeslami

B.A.Sc., Simon Fraser University, 2014

Thesis Submitted in Partial Fulfillment of the
Requirements for the Degree of
Master of Applied Science

in the
School of Mechatronic Systems Engineering
Faculty of Applied Sciences

SIMON FRASER UNIVERSITY

Fall 2019

Approval

Name:	**Sepehr Sheikholeslami**
Degree:	**Master of Applied Science**
Title:	**Soft Gripper Driven by a Solenoid Actuator**
Examining Committee:	**Chair:** **Helen Bailey** Lecturer
	Carlo Menon Senior Supervisor Professor
	Flavio Firmani Supervisor Lecturer
	Woo Soo Kim Internal Examiner Associate Professor
Date Defended/Approved:	November 28, 2019

Abstract

In the past thirty years, robotics technology has become well-established in the manufacturing industry for reducing worker ergonomic stress and workload by performing operations such as picking and placing objects from a location to another, quickly, repetitively, and accurately. As we continue to integrate robots as versatile aids for industry, it is important to develop mechanisms that facilitate seamless cooperation between humans and robot assistants (RAs).

Contributions of this thesis include the design and development of a more advanced, yet simple and cost-effective soft industrial robotic gripper that is scalable, and can be mounted on a wide range of commonly used robotic arms. The finished gripper prototype uses inexpensive components, and thus, would be economical to produce while addressing the needs of industry.

Depending on the application, the developed gripper can outperform the state of the art in many “pick and place” tasks and is capable of picking up a wide variety of objects in size, weight, geometry and texture. To be applicable to current industrial warehouse environments, a series of tests were conducted to evaluate the effectiveness of the gripper in picking up and placing a set of items commonly available. The developed gripper in this work was mounted on a KUKA arm, and was tested for gripping objects from delicate ones such as a light bulb to heavier ones such as a 23 cm x 14 cm x 12 cm pack of eight cans of soda, weighing around 3 kg with a measured speed of 0.88 m/s.

Keywords: Soft robotic gripper; polymer membrane; delicate objects gripper; variable-volume chamber; flexible silicone membrane; magnetic gripper

To my family for their indefinite support through all my life

Acknowledgements

I would like to thank my senior supervisor, Dr. Carlo Menon for his understanding and help since day one I started my research. He was the main reason I have start this research and I am where I am today with this project.

I would also like to thank past and present members of MENRVA research group who have helped me throughout my research.

Finally, I would like to thank my parents and sister who encouraged me in taking this path and supported me through all these years. The only reason I reached to this point in my life is my parent's moral and financial support.

Table of Contents

Approval ii
Abstract iii
Dedication iv
Acknowledgements v
Table of Contents vi
List of Tables vii
List of Figures viii
List of Acronyms x

Chapter 1. Introduction 1
1.1. Background and Motivations 1
1.2. Objectives 3
1.3. Thesis Layout 4

Chapter 2. Literature Review 5

Chapter 3. Design Considerations 10
3.1. Gripper Configuration 10
3.2. Gripper actuation 27
3.2.1. Solenoid Actuation 27
3.2.2. Coil Experimental Investigation 32
3.2.3. Solenoid Model 38
3.2.4. Solenoid Model Verification 40
3.2.5. Solenoid Design Consideration 41
3.2.6. Solenoid Optimization 45
3.3. Gripper Soft Membrane 50
3.4. Gripper Electronics 57

Chapter 4. Testing and Experiments 61
4.1. Peak power of the gripper 61
4.2. Force Measurement 63
4.3. Actuation Speed 66
4.4. Picking up Objects with Different Shapes and Weights 66

Chapter 5. Conclusion 70

References 72

List of Tables

Table 1: Comparing different versions of the gripper at a glance.....21
Table 2: Different 3D printing methods and their respective material data.....26
Table 3: Prototyped coil and magnet actuator.....40
Table 4: Constant parameters for the coil and magnet.....47
Table 5: The Best, Average, and worst Function value obtained using GA, SA, and PS. α, β, and dw for best value are only written in the table. 48
Table 6: Polymer Characteristics [94].....51

List of Figures

Figure 3.1: gripper's three main components. Half of the membrane is only shown to illustrate the magnetic shaft....11
Figure 3.2: Gripping process....13
Figure 3.3: Gripper’s different prototypes and their cross-section view....14
Figure 3.4: Membrane Installation for versions 2-4....16
Figure 3.5: Assembly to make a custom coil on a custom bobbin....18
Figure 3.6: Forcing the inflated membrane toward the object by using a clip around the gripper....19
Figure 3.7: Final version of the gripper with its shaft is extended and its cross section....20
Figure 3.8: Gripper's body attached to a rotary tool for wrapping the coil....20
Figure 3.9: Exploded and isometric view of the gripper in SolidWorks....23
Figure 3.10: Sealing Membrane to the shaft....24
Figure 3.11: Overexposure of an ABS part to acetone vapor....25
Figure 3.12: Pictures of different stages of gripping an object....27
Figure 3.13: Cross Section of a solenoid made of a coil and a permanent magnet shaft....28
Figure 3.14: Force sensor attached to a leveling device....29
Figure 3.15: Shaft comparison between a solid fill cobalt steel cylinder, a hollow cobalt steel cylinder with 21 mm inside diameter, a solid fill rare earth magnet, and a hollow rare earth magnet with 12.7 mm inside diameter....30
Figure 3.16: Cross section of an energized coil and a set of permanent magnet shafts....31
Figure 3.17: Cross section of a pair of identical coils with two different size magnets 31
Figure 3.18: Actuation force with respect to displacement of the magnetic shaft to the coil....32
Figure 3.19: Comparing actuation force when doubling coil length and keeping everything else constant....33
Figure 3.20: Comparing actuation force when two shafts with different diameters are used and all other parameters are kept constant....34
Figure 3.21: Comparing actuation force when two shafts with different lengths are used and all other parameters are kept constant....35
Figure 3.22: Comparing actuation force when two coils with different lengths are used and all other parameters are kept constant....36
Figure 3.23: Comparing three custom wrapped coils using different wire gauges....37
Figure 3.24: Geometrical parameters of the coil and magnet actuator (modified from [80])....38
Figure 3.25: Comparison of analytical and measured force values using the designed gripper....41
Figure 3.26: Normalized force vs center to center distance for different coil ratios....44

Figure 3.27: Normalized force vs center to center distance for different magnet ratios 44
Figure 3.28: Optimized Normalized Force vs Coil's wire diameter 50
Figure 3.29: Shore Hardness scale (Modified from [95]) 52
Figure 3.30: Injection molding prototype to create silicone membrane. a) Full assembled mold, b) Mold inner shell 52
Figure 3.31: EcoFlex™ 00-10 created using an injection molding method 53
Figure 3.32: Different Silicone mold iteration. Silicone was applied using a brush in these molds 54
Figure 3.33: An injection mold Similar to the model of a wine bottle 56
Figure 3.34: Final Mold prototype 56
Figure 3.35: Control Box Wiring Diagram 58
Figure 4.1: Peak Power of the gripper. Stages 1 and 4 peak powers are negligible, but stage 2 can be different depending on the current applied. 2.5 A, 1.8 A, and 0.87 A are shown. 62
Figure 4.2: Force Measurement test setup 63
Figure 4.3: A rubber ball with a tube inserted to create a hole 64
Figure 4.4: Force measurement results 65
Figure 4.5: Gripping Force VS Gripper's input peak power 65
Figure 4.6: Gripper actuation speed vs input power 66
Figure 4.7: Picking up objects with various shapes and weights. 68
Figure 4.8: Gripping various objects and a picture of their contact point with the gripper 69

List of Acronyms

ABS	Acrylonitrile butadiene styrene
AWG	American wire gauge
CAD	Computer-Aided Drafting
CNC	Computer Numerical Control
CPU	Central Processing Unit
DEA	Dielectric Elastomer Actuator
DOF	Degree of Freedom
FDM	Fused Deposition Modeling
FEA	Fluidic Elastomer Actuator
GA	Genetic Algorithm
ID	Inside Diameter
KUKA	Keller und Knappich Augsburg
OD	Outside Diameter
PS	Pattern Search
RAs	Robot Assistants
SA	Simulated Annealing
SFU	Simon Fraser University
SLA	Stereolithography
SLS	Selective Laser Sintering

Chapter 1.

Introduction

This chapter starts with explaining more about the background and motivation for researching a soft gripper in **section 1.1**. It then lays out the objectives for this thesis in **section 1.2**. In **section 1.3**, the layout for the rest of chapters in this thesis is presented.

1.1. Background and Motivations

Factories have automation systems for all kinds of tasks such as assembling cars, sorting and packing food or medicine, or working alongside human for doing complex and precise tasks. A necessary part of production industry has been robots starting 20th century [1]. The rise in population creates the need for using more robots and automated manufacturing. Robots are already being used in factories to replace humans in doing jobs such as repetitive, hazardous, or dirty ones [2]. Using robots increases both the product quality and the factory's profitability. Some precise and small parts assembly tasks require more robots to be used in assembly lines. Hence collaborative robots to work alongside humans become attractive due to both the limited space in factories and higher flexibility in assembly lines [3]. This need is specially more attractive in industries with frequent product change like consumer electronics [3]. Hence, due to the limited space in factories and variability of tasks, some robots will have to work alongside human or be guided actively by human [4]. The cooperation of human and robots can increase the productivity of assembly lines and reduce the number of breaks and exhaustion. In one assembly line, robots can handle the repetitive simple tasks and human can handle more complex tasks [4].

Increasing need for using robots to collaborate with human and do human tasks that normally require handling with hands, brings more attention toward robotic grippers [5]. Robotic grippers have been used in numerous applications, such as surgical operations [6], or industrial use where robots are used to increase production capacity [7]. UNIMATE industrial robot was the first robot used in an assembly plant in 1961 [7], and ever since many companies have researched and industrialised grippers with various drive mechanisms [7]. Another application of robotic grippers is in gripping fragile objects

by incorporating various sensors [7] such as force feedback sensor to control the pressure applied by the robot and not damage the object being picked like grippers for food industry [8].

In general gripping process is achieved by gripper approaching the object, contacting the object either physically or by a force field generation, securing the object by increasing the force of the gripper, moving the object, and finally releasing it [9]. Different grasping methods have been developed during the past decade to pick objects ranging from big and heavy ones to micro size objects. Some of these grasping principles are mechanical grippers which are widely used in the industry, electrostatic grippers to manipulate and assemble micro structures [10], or Bernoulli grippers which work with the concept of air flow [9]. Research in grippers have evolved impressively in recent years, hence new challenging grippers such as adaptive grippers or grippers using smart material are being studied and developed [7].

One interesting field that is drastically improving, is the field of soft grippers to handle delicate objects such as fruits [11]. In contrast to most manufacturing robots which are stiff so that they can perform fast and precise operations, soft grippers have a soft and deformable end effector to interact with objects [12]. Some soft grippers that has been recently developed are inspired by animal body structure, such as grippers having a sac filled with granular material and using vacuum pressure to jam the material for gripping [13], [14], or a soft robot gripper based on octopus structure [15]. Most commercially available grippers have limits such as the need to use an external vacuum pumps for actuation [13], or not having enough gripping speed. Hence, comes the need for robots that are fast and versatile, so they can be easily used by any person and does not need complex structure to set them up.

The gripper should have a velocity suitable for collaborative robots. For instance, OnRobot has three commercially available grippers called RG2, RG6, and RG2-FT with maximum gripping speeds of 127 mm/s, 160 mm/s, and 184 mm/s respectively. These robots were specifically designed for collaborative robots. The proposed gripper should therefore have a similar velocity (e.g. 0.2m/s) [16].

1.2. Objectives

The present work is about designing a gripper that can pick and place various objects such as delicate ones like fruits without damaging them. The gripper is intended to have strong gripping force, fast actuation, yet soft to interact with wide range of objects. Based on these requirements, this thesis has 2 main objectives.

Objective 1 is to design and fabricate a soft gripper which is:

a) Compact (i.e. have about the same size volume of a gripper used for collaborative robots)

b) Able to grasp objects having different shapes

Objective 2 is to design an actuator for the proposed gripper that:

a) Does not require external actuation source (e.g. pressured air line)

b) Has a velocity higher than 0.2 m/s

c) Generates a force suitable to grasp lightweight and medium weight (e.g. <4 kg) objects

1.3. Thesis Layout

Chapter 2 is a literature review of robotic manipulators and then it is narrowed down to wide range of robotic grippers, and then it is further narrowed down to soft grippers.

In **chapter 3**, the gripper design and electronics are explained to meet both **objective 1** and **objective 2**. Each sub section in this chapter gives detailed explanation about each main component to make a working gripper ready for measurement and testing.

Chapter 4, investigates functionality of the gripper by doing some testing and evaluations to confirm achievement of **objective 1** and **objective 2**. Each section shows the result of evaluations done on the finalized prototype. At the end of chapter, some pictures of an actual test using a KUKA robot to pick and place wide range of objects is shown.

Chapter 5 concludes this thesis and explains how the objectives of this work are met.

Chapter 2.

Literature Review

This chapter does a detailed literature review about robotic manipulator and then narrows down to robotic grippers and soft grippers.

Robotic research existed for at least 100 years. After some development in designing robots, the need for robotic manipulator arises. Developing dexterous robotic manipulators started roughly about 58 years ago [17]. Many robotic hands were developed with different actuation systems, and all had their own advantages and disadvantages. Depending on different applications different robotic hands were developed. But developing more advanced anthropomorphic robotic hands started about 25 years ago [18]. Based on application of the robot hand, different design parameters such as degree of freedom (DOF) and number of actuators need to be defined. The preference is to achieve more DOF with less actuators, and the preferred method of actuations are electric, pneumatic muscles, and pneumatic cylinders at 75%, 19% and 6% respectively [18]. Most electronic grippers basically have their main components to be motors, sensors, and a controller to regulate the actuation depending on readings of the sensors.

Anthropomorphic grippers are categorized as active grippers imitating human hand in gripping objects [19]. A good example of an anthropomorphic gripper is the DLR Hand Arm System that has about 19 DOF in total and 52 motors [20]. To mimic the functionality of a hand, these grippers need to have a high DOF which leads to the need for algorithms to control the grasping motion of grippers with multi-fingers [21], [22] and this adds complexity to the system [23].

Robots are used mostly for repetitive job in the industry. Grippers are the end tool for robots in handling objects. With the need to pick different objects comes the need for flexible grippers. Typically, in production lines each gripper is made specifically for a specific type of product, and it needs to be modified to handle a different item [24].

Most of the grippers in the industry are created for specific tasks either complex or simple. But these grippers are not designed to adapt to the shape of different objects. Therefore, there is a need to create more adaptable grippers to grasp a wide range of

objects rather than just a specific one [25]. One approach is to design underactuated grippers meaning they have more DOF than the number of actuators. Therefore some other means of passive parts are used with these grippers to achieve the gripping goal [26]. Some underactuated grippers have been studied with fingers to adapt to an object's shape both with rigid and soft gripping fingers [27]–[30]. For instance, a compliant underactuated hand was designed with three fingers and five actuators in [31]. This robotic hand was designed with the main goal of being simple and inexpensive, yet capable of gripping different objects [31]. It has been shown in the literature that underactuated grippers require a much simpler algorithm than more complex grippers and they can perform more grasping variations [25].

In order to achieve the goal for more flexible grippers, numerous studies have been done on grippers which can pick and place objects with different shapes and weights. Most of these grippers are categorized as passive grippers [19]. These types of grippers have a passive gripping element like an elastic element which conforms around the object being picked. The formation of the elastic element can be done by various methods. one method is using a combination of negative and positive pressure inside a sealed gripper to jam material in the gripper [13]. Other approaches of passive grippers can be using a pneumatic actuator and a series of chambers embedded in elastomers [32], [33], hydrostatic skeleton [34], suction based [35], [36], and much more.

Passive grippers that have a soft, usually elastomeric, material can be subcategorized into soft grippers. Soft grippers can grab the object being picked by actuation, controlled stiffness, or controlled adhesion [37] of the elastomer. Soft grippers usually have much less complex control system due to their mechanical design and the soft membrane.

One of the main advantages of soft grippers is the simple design in compare to active grippers mentioned earlier. Some of these grippers need a vacuum pump to actuate. For example, jamming grippers are filled with granular material covered with an elastomer. Their membrane forms around the object being picked, and the air inside is evacuated to make it rigid. Hence picking up the object [38]. Some other researchers have used vacuum pumps for fairly long time, where they use tips like suction cups to seal the membrane of the gripper on the object and create a suction to pick it up [39], but they mostly work with deformable and lightweight objects [24]. Some soft grippers have a

tendon structure and by inflating the manipulator they can move around an object and perform the gripping task similar to an octopus [40].

An interesting application for soft grippers is to use them in the food industry. Food products can have a wide range of shape and roughness, and most of them can easily get damaged if an excessive force is applied in the process of picking them [41]. They require delicate handling and still rely heavily on human to handle individual items [42]. Different grippers have been studied to handle fragile food items such as fruits [43], [44]. Some researchers have also developed grippers to handle food objects that are highly deformable. For example, a gripper was developed in the literature incorporating a bellow type soft actuator being able to grasp a wide range of food object with a wide opening in an idle stage yet compact [45].

Most soft grippers have their membrane made of silicone since they can be easily manufactured and have a low mechanical damping coefficient [37]. For example, they are used in fluidic elastomer actuator (FEA) designs where they restrict the structure of the actuator, so that one part is stiffer than the other, hence by changing the internal pressure they will be able to move the actuator to the desired direction [46]. This method has been used to create multi-chambered fingers for grasping objects [47], [48]. Over the time they recreated the same concept with self-healing membranes [49]. Other researchers have extended the use of FEA by combining conductive and dielectric silicones to create dielectric elastomer actuator (DEA), where an electric stimulation deforms the polymer [50]. Some researchers saw interest in creating a controlled adhesion between the surface of the gripper's membrane and the object being picked [51] which is inspired from gecko. Further developments lead to electro-adhesion which is based on the attraction between positive and negative electric charges where in one case a dielectric object is charged that is polarized and in another case a conductive object has electrostatic induction due to the electric field applied [37]. These grippers can grasp and manipulate soft objects [52]–[54]. Some other soft grippers have a single or multiple soft structures that are similar to fingers or octopus legs [55]. Most of the soft grippers with this structure perform the grasping procedure either using a pneumatic actuator or tendons attached to the part [56]. To better illustrate, pneumatically driven ones have channels embedded inside the soft structure and this soft structure is deformed and grasping is performed by applying pressure inside the channels. In the other case, cables with different length similar to tendons with variable

lengths are connected to the gripper [57] on one end and connected to motors on the other end.

A number of soft robotic grippers have been researched academically and some of them were launched commercially [58]. Soft Robotics is a soft gripper that is currently selling in the market incorporating soft fingers actuated pneumatically [59]. Festo developed FlexShapeGripper which is another soft gripper heading to the market having its grasping principle inspired by a chameleon [60].

The goal of this work is to design, develop, and evaluate a robotic gripper that can pick and place a wide range of objects such as delicate objects like fruits without damaging them. There are numerous grippers in the market with different actuators that are either integrated in the gripper itself or are external actuators. Some grippers use motors as actuation [19] to perform the gripping action. Some use vacuum pumps to create a seal between the gripper and the object using a vacuum cup [61], and some use vacuum pumps to jam granular material formed around an object [13]. Also external devices have been used in some grippers to inflate chambers inside a shell to create movements of this shell by inflating these chambers [62]. However, the gripper proposed in this work is more appealing than existing grippers in the market due to its simple mechanical and electrical design, yet strong gripping force. To achieve a more optimal actuation speed than other common grippers in the market such as those that use motors or vacuum pumps to perform the gripping action, a solenoid actuator was developed to run the gripper. This further allows the gripper to be self-contained, and not requiring any special equipment such as air compressor or vacuum pump to operate.

Electromagnetic actuators are normally cheaper and need much simpler control algorithms than other actuators [63]. Normally electromagnetic actuators have a movable part which is called a shaft or rod, and this shaft can be an iron, permanent magnet or even a coil by itself. The movement of this shaft is normally achieved by using one or two coils and energizing them [64]. Conventional solenoids have a coil and an iron shaft. The coil is energized and its magnetic field moves the shaft in one direction [65]. In some cases a spring is used to move the shaft to its original position after the current applied to the coil is turned off.

Some rigid grippers have been designed using a solenoid as the actuator for their grippers. For example mechanical movement of grippers with gripping fingers can be operated using a solenoid, where two fingers are opposing each other and connected to the piston of a solenoid. The position of these fingers can be changed by actuating them through moving the piston inside the coil of this solenoid [66]–[68]. Linear solenoid actuators have been used in the industry for different applications such as actuating mechanical components of a robot [66], quick latching mechanisms where a fast transition time is required in actuation [69], or simple on/off valves [70].

I order to increase the electromagnetic force of a solenoid, the iron shaft in the middle of the coil have sometimes been changed by a permanent magnet. Since the permanent magnet itself is magnetized, the solenoid with a permanent magnet shaft is bi-directional [71]. Solenoid actuators with the permanent magnet shaft have been developed in the past [64], [65], such as miniature solenoids for valve mechanisms [72], [73].

Chapter 3.

Design Considerations

This chapter aims to tackle both objectives of this work. The overall configuration and the Computer-aided drafting (CAD) design of the gripper is presented in **Section 3.1** showing a gripper that is fast and compact in size to tackle **Objective 1**. To meet **Objective 2**, the actuation method implemented on the gripper along with the tests, designed and conducted to validate and justify the method are discussed in **Section 3.2**. **Section 3.3** details the developed prototypes leading to the final design of the soft membrane used on the gripper, and **Section 3.4** illustrates the electronics wiring diagram of the gripper.

3.1. Gripper Configuration

Today, the predominant robotic form factor used in warehouse industry is that of single-arm robotic manipulators with grippers attached to them. While the existing grippers could be very efficient at completing the limited tasks they are designed for, they tend to be slow, inefficient and even inapplicable to other gripping tasks [37]. Therefore, to bridge the gap between current systems and future robot embodiments, this thesis focuses on the design, development and evaluation of a robotic gripper that is capable of gripping and picking up a wide variety of objects commonly observed in warehouse environments, ranging from small and delicate objects such as a light bulb to much heavier ones like a 3.5 kg fire extinguisher. In this section, we detail the gripper's design along with the stages of the gripping process.

To address the current needs of the industry, the designed gripper has fast actuation, while maintaining a small size so it can reach into tight spaces if necessary. Further, a soft membrane is incorporated on the outer surface of the gripper, allowing the gripper to comply to the specific object's geometry being picked without damaging it. Also, the designed gripper is self-contained, and does not require any additional equipment such as a vacuum pump or an air compressor to function.

The developed soft gripper has a simple mechanical and electrical design, and is more appealing than its existing state of the art (e.g. [19], [61]), since it is less costly to

rescale and produce, and can be mounted onto existing robots without any replacement of electrical or mechanical components.

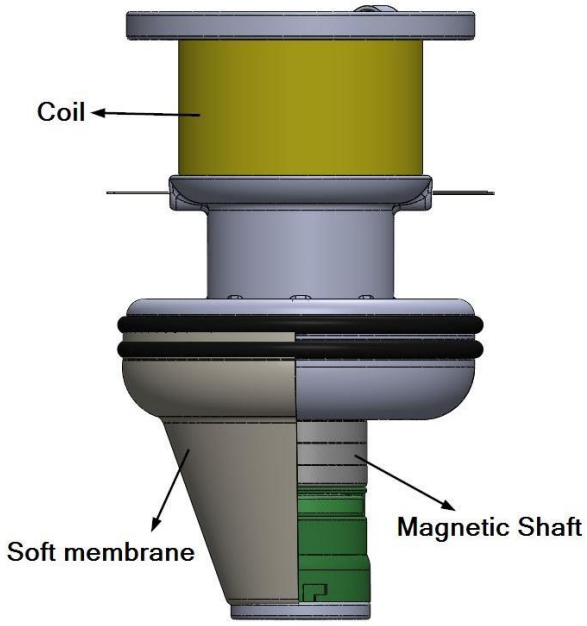

Figure 3.1: gripper's three main components. Half of the membrane is only shown to illustrate the magnetic shaft

The gripper is comprised of three main components: a coil, a magnetic shaft and a soft polymer membrane, see Figure 3.1. The gripper is designed with a chamber inside that is connected to a miniature actuated on/off solenoid valve from the top. The chamber is sealed with a conical shaped flexible membrane that holds the magnetic shaft which is otherwise detached from the gripper's body. Hence, when the gripper is mounted on a robot arm, the shaft is suspended from the polymer membrane (Figure 3.1).

The gripper's soft polymer might have to be changed due to sharp objects accidentally damaging it. To address this issue, the gripper is designed such that changing a membrane is easy and takes the minimum time and effort to replace. Changing membrane on this gripper is much faster than previous designs we had (which would take about 45 minutes [19]) and it only takes less than 1 minute and simply an Allen key tool is required.

The gripper's fundamental gripping mechanism is based on the following formula, assuming there is no leakage (Boyle's law):

$$P_f = \frac{P_i V_i}{V_f} \tag{1}$$

where i denotes the initial value and f denotes the final value for pressure and volume.

The gripping mechanism relies on the suction as well as the friction created between the gripper's membrane and the object being picked, and occurs in a transition of following stages following Boyle's law shown in equation 1, (Figure 3.2):

1) The robot approaches the object (Figure 3.2-a) until the magnetic shaft, suspended from the gripper's body, hits the object (Figure 3.2-b);

2) As the robot descends, the reaction force exerted from the object causes the shaft to retract inside the sealed chamber. The volume drops considerably inside the chamber to compensate for the volume occupied by the shaft, creating a significant amount of positive pressure inside the chamber. This pressure inflates the membrane and seals it around the object being picked. (Chamber volume is shown in red color in Figure 3.2. Initial volume (V_i) of the chamber is shown in Figure 3.2-a in red, where the shaft is fully extended and the membrane looks like a truncated cone. The final volume (V_f) of the chamber is shown in Figure 3.2-d in red, where coil is on and the shaft is in fully retracted position.)

3) The robot continues descending and the shaft continues retracting inside the chamber until it occludes the field of view of the infrared sensor (Figure 3.2-c).

4) Then the robot arm stops moving, and the sensor activates the solenoid actuator, moving the shaft further inside the gripper's body. This mechanism not only increases the positive pressure inside chamber for a better seal (shown in red), but also results in a strong suction force between the shaft and the object being picked. (The portion related to suction volume is shown in blue in Figure 3.2. There is a negligible initial volume (V_i) between the object and the shaft shown Figure 3.2-c in blue. After the shaft fully retracts as shown in Figure 3.2-d, the final volume (V_f) between the object and shaft increases (shown in blue) creating suction.)

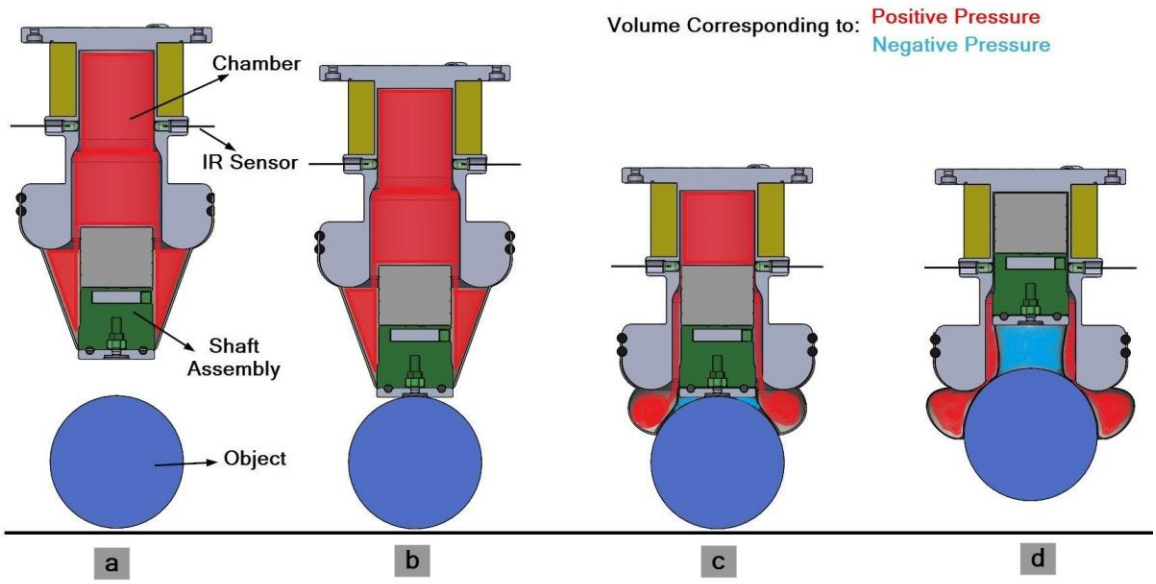

Figure 3.2: Gripping process

To achieve the optimal gripping performance, different prototypes were designed and tested. The evolution of these different prototypes was based on force of a coil as an actuator to have the ideal power needed for actuation, changing volume ratio of different gripper components to achieve the necessary force to grip the object being picked, and the air gap created between the gripper's shaft and the object to create a strong suction. This gripper had 6 different prototypes versions and they are all shown in Figure 3.3. Version 6 is the final version. Please note that all grippers in Figure 3.3 are shown in fully retracted position without any membrane attached.

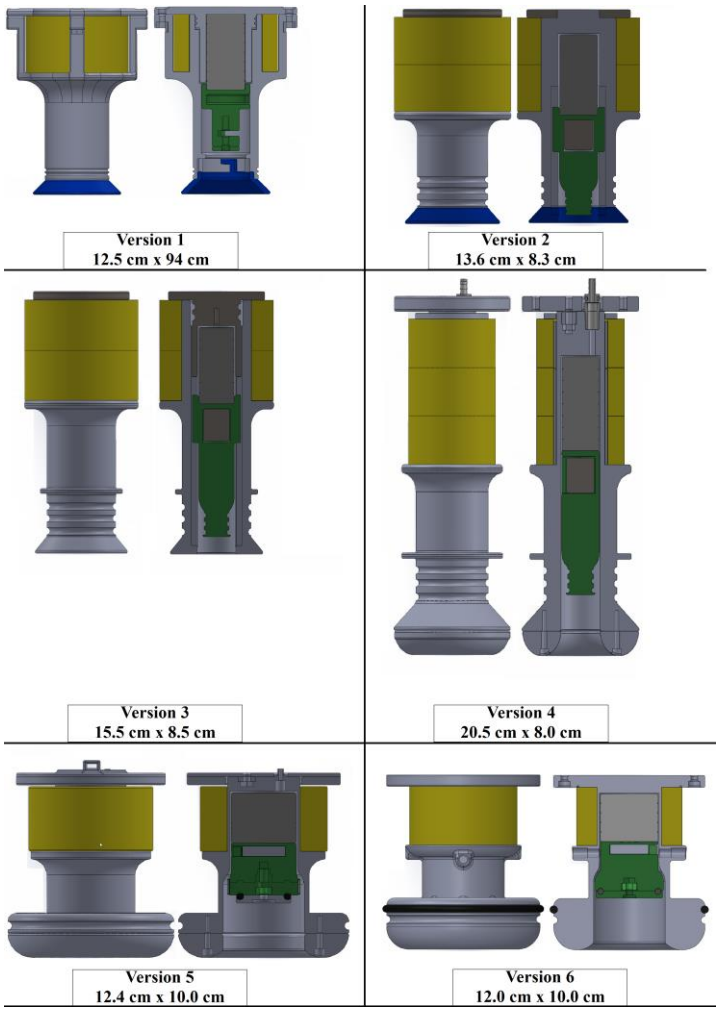

Figure 3.3: Gripper's different prototypes and their cross-section view.

All different versions of this gripper were improved and evolved one after another. Three main objectives were considered when the gripper was being designed an improved. One objective was to have a strong actuation force, another objective was to design the gripper to maximize the positive pressure inside the chamber when the shaft is retracted, and the last objective was to increase the suction between gripper's shaft and the object being picked. In creating all these versions, I have mainly focused on changing the physical dimension of the gripper's body and its components such as the coil and the shaft.

Version 1 was using a single coil with 50.8 mm inside diameter, 82.6 mm outside diameter, and 29.5 mm height, while versions 2 and 3 had 2 of the same coil attached together in series with an effective height of 59 mm. This improvement was done to increase the stroke in the gripper and hence both increase the actuation force and the

positive pressure inside the chamber. Also the idea of using a hollow truncated cone (the blue piece shown in Figure 3.3, Version 1) or a partly filled truncated cone (the blue piece shown in Figure 3.3, Version 2) was to have these pieces removable for testing and make sure that they can improve the gripping force. Then it was finalized in version 3 and added as a permanent piece. Use of the partially filled truncated cone helps optimize the volume ratio inside the chamber when the shaft is extended and retracted and increases the positive pressure inside the chamber when the shaft is retracted. This truncated cone's diameter can also be changed to make the gripper's opening bigger or smaller based on the needed application and objects being picked. In all these three versions there was a mechanical stop created to prevent the shaft from travelling out of the gripper's body.

In version 1, the membrane was simply sandwiched between the shaft tip and another flat thin cylinder, but this idea was both leaking and damaging the membrane around the edges of the shaft. All gripper versions have a 3D printed shaft (the green piece shown in Figure 3.3) using Acrylonitrile butadiene styrene (ABS) plastic to connect to the membrane. In all version the 3D printed part of the shaft has a cavity to hold a magnet to fix the main magnetic shaft (the gray piece shown in Figure 3.3) to the 3D printed part of the shaft.

In versions 2-4, the membrane used for gripper was a party balloon. One end of balloon was attached to the shaft using O-rings, and the other end was attached to the gripper using bigger O-rings. In order to reduce the leakage in gripper, one small piece of balloon (red balloon in Figure 3.4-(a) and the yellow balloon in Figure 3.4-(b)) was first attached to the shaft using an O-ring as shown in Figure 3.4-(a); then the main membrane (orange balloon in Figure 3.4-(b)) was attached to shaft using two O-rings (Figure 3.4-(b)) at the balloon's stem. Some expanding glue was added between the 2 balloons to further reduce the leakage in gripper.

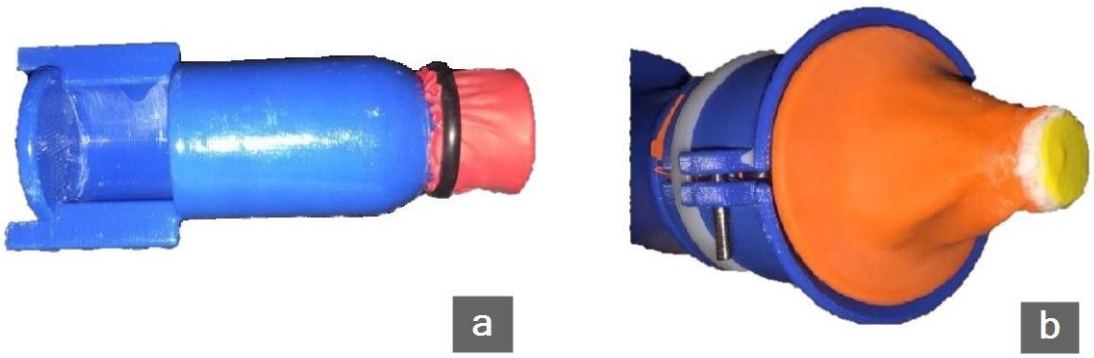

Figure 3.4: Membrane Installation for versions 2-4

Version 4 was changed to incorporate a longer stroke, hence having a longer coil (3 coils were attached together in series to form a single coil). Having a longer stroke would increase the suction volume created between the object and the shaft and consequently it would increase the suction force. The gripper opening was also slightly increased to cover bigger surface area when picking objects. This would help specially with cases like fruits (having a stem on top) where the stem had to be covered completely to prevent any leakage. A half toroid piece was also added at the bottom of gripper to better optimize the volume ratio, creating a higher positive pressure inside the chamber. This half toroid adds a constant volume to both initial and final chamber volume, hence increasing the positive pressure and causing a stronger seal created by the membrane on the object.

Starting from version 4, a valve connector was added to connect a solenoid actuated valve to the gripper. This valve was located on the top in versions 4 and 5, and it was located on the side in version 6. Solenoid actuated valve was responsible to neutralize the gripper's chamber pressure when the gripper is in idle mode and shaft was extended. Since the gripper could not be 100% leak proof, the air slowly leaked every time the chamber was retracted and positive pressure was built. In other words, the gripper's pressure became negative instead of neutral pressure when the shaft was extended again and the solenoid actuated valve would help to neutralize that. The volume ratio is constant when the shaft was retracted or extended. Therefor if there was a leakage when the shaft was retracted and positive pressure was created, then that same amount of air leakage would be reduced from the initial pressure when the shaft was back to extension and would cause a negative pressure instead of neutral.

In versions 1-3 a mechanical stop was designed to prevent the shaft from moving out of gripper's chamber. There were also 2 small groves on sides of the chamber to guide the shaft and prevent twisting. But starting from version 4, these side grooves were removed to further increase the positive pressure inside the chamber when the shaft was retracted. The mechanical stop at the bottom of gripper was also removed, so the shaft can be inserted from the bottom rather than the top of the gripper. An advantage of removing this mechanical stop and side grooves was that it would reduce the leakage by eliminating the need to seal the top of gripper shown in versions 1 and 3.

In version 2, shaft was also inserted in the gripper's chamber from the bottom, but then the bottom cone had to be assembled, which was added later as a solid piece merged with the gripper's body. Most of the parts in these different gripper versions, were design to be removable, allowing for more tests in different gripper geometries. For example, the bottom truncated cone was removable in versions 1 and 2 and then it was merged as a solid with gripper's body in the later designs since it was proved useful for the gripper. Another piece that was removable first and then added as a solid piece was the bottom half toroid which was removable in versions 4 and 5, and the merged with gripper's body in version 6.

Gripper versions 1-5 were all made in a way to be able to insert a commercially available coil on them. In order to test some coils with different parameters and experiment with them, some were purchased from a company called APW Company [74]. Coils are shown in yellow color in Figure 3.3, and it is clear that versions 1-5 have a removable cap to be able to insert these different coils and test them. More detail on coil experiments is explained later in section 3.2. Versions 1-4 were all using premade coils for from APW, but then starting from version 5, coils were manually made by hand and tested on the grippers. Figure 3.5 shows the assembly to make a coil and insert it on version 5 gripper. The grey part shown in Figure 3.5-(a) tightens to the blue bobbin shown in Figure 3.5-(b) and the single screw on top attaches to a drill to wrap wire around the bobbin.

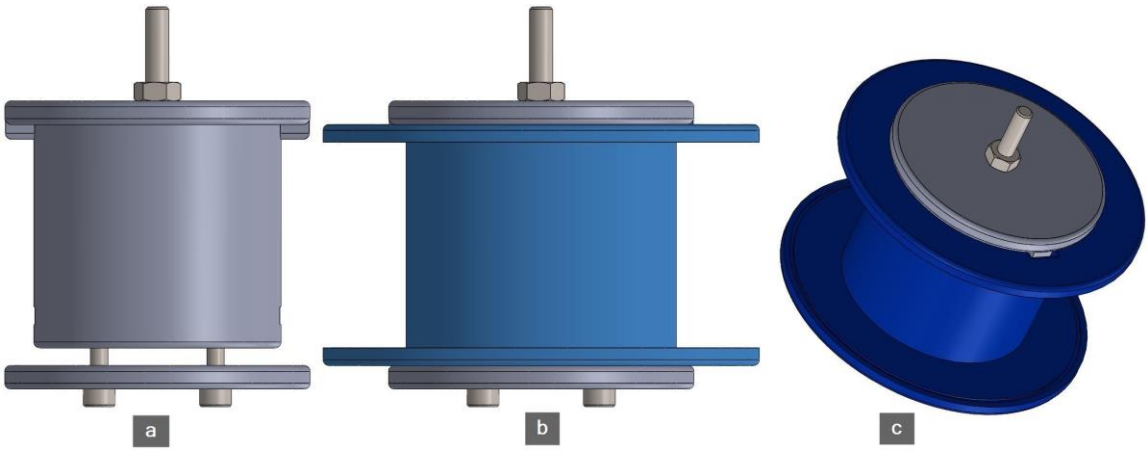

Figure 3.5: Assembly to make a custom coil on a custom bobbin

Version 5 dimensions were considerably changed to accommodate for bigger diameter magnetic shaft. A bigger magnetic shaft was decided to be added to increase the actuation force of the gripper and it will be further explained in section 3.2. Different shaft sizes (the green ABS part) were printed and tested. Since the shaft tip area was increase, the surface area to create the suction between the gripper's shaft and the object being picked was also increased, therefore the length of the gripper could be reduced to make it more compact, keeping the same initial and final volume ratios.

A major change in version 5 was the chamber design modification. The chamber was no longer a continuous cylinder like versions 1-4, and it had a wider opening from almost half way down. There were two advantages to this design change. One was that the plastic piece of the shaft could be made even bigger than the magnetic part which would increase the suction force, and the other advantage was that the shaft could tilt slightly. Since the shaft was suspended over the membrane, it could slightly tilt in the wider opening of the chamber at the start of the gripping action. In other words, the gripper did not need to perfectly sit on the center of an object being picked. The shaft could tilt at the beginning and it would straighten up as the gripper moved further down on the object and the shaft moved further inside the chamber. Another major change in version 5 was the method of attaching the membrane to the ABS piece of the shaft. Instead of using 3 O-rings like the previous method which was shown in Figure 3.4, the membrane attached to shaft using only one O-ring and it was done much faster than the previous method. One end of the membrane simply got sandwiched between shaft and a plastic tip that tightened to shaft using a screw. Since this shaft was bigger than the one in version 1, we could use

an O-ring in between the two flat surfaces for a better seal, and it did not have pressure points on membrane to damage it.

After a few tests with version 5, it was noted that the built-up positive pressure inside the chamber was being wasted by inflating the membrane in the direction that was not useful. Therefore, a temporary cardboard ribbon was added around the gripper to focus the membrane inflation in the right direction which was toward the object. Figure 3.6-(a) shows how the inflation was all around the gripper and covering a small portion of the apple. But Figure 3.6-(b) shows the desired inflation by using a ribbon around the gripper and guiding the membrane inflation toward the same apple used in Figure 3.6-(a). Having more surface area of membrane around the object created a stronger friction between gripper and the object, and it also reduced the chance of leakage in the volume creating suction between the shaft and the object.

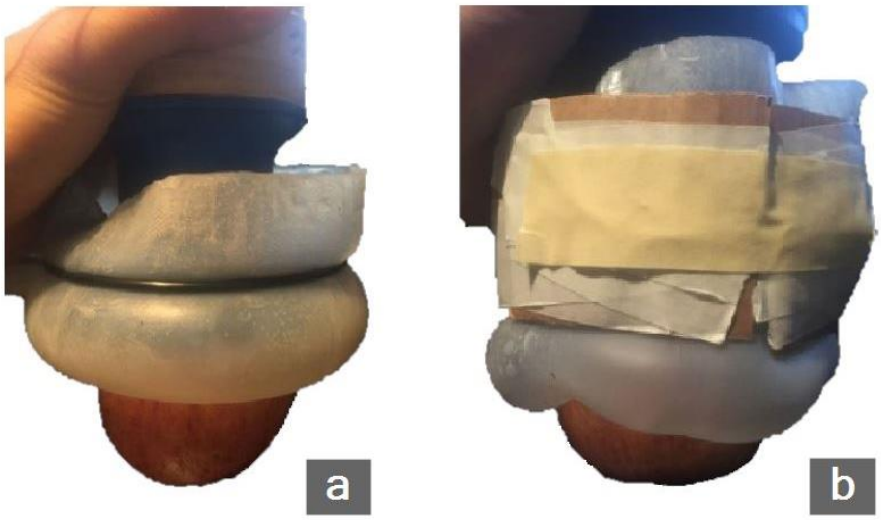

Figure 3.6: Forcing the inflated membrane toward the object by using a clip around the gripper

Version 6 shown in Figure 3.3 had some minor modifications for the finalized design and better performance, but none of the core design factors such as the gripper dimensions, the coil or the shaft size were changed. The half toroid on the bottom of the gripper in version 5, which was removable, was then merged as a solid body with the gripper's body. The valve connector for solenoid actuated valve was moved to the side, so we could reduce the height further and easily connect the gripper to KUKA robot arm end effector without the valve interfering. Two holes were also added in the gripper's body to insert an infrared receiver and an infrared emitter. Infrared sensor detects the presence

of the shaft and activates the coil. Figure 3.7 shows the finalized gripper with membrane attached when the shaft is fully extended.

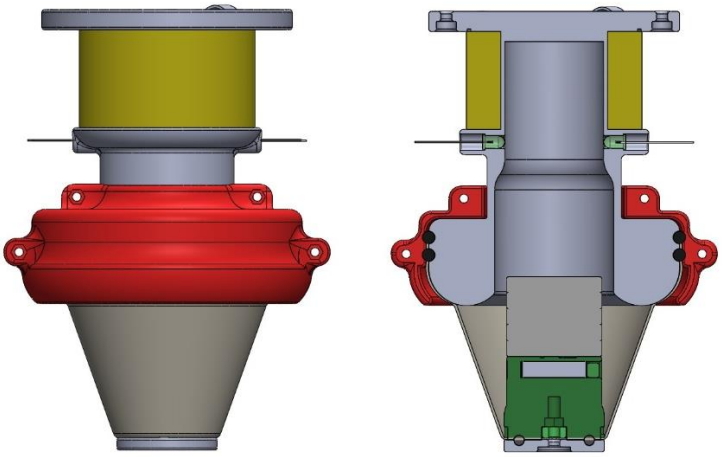

Figure 3.7: Final version of the gripper with its shaft is extended and its cross section

The coil in version 6 was wrapped directly on the gripper's body, hence the top piece plate of the gripper was also merged as a solid body with gripper's body. By wrapping the coil directly on gripper, the gap between coil and magnetic shaft was reduced to 1.5 mm, which effectively increased the actuation force of the gripper. An extra attachment was made using a 3D printer to fix the gripper's body to a rotary tool to make the wrapping faster and easier. Figure 3.8 shows the gripper attached to a rotary tool and ready for wrapping coil wire.

Figure 3.8: Gripper's body attached to a rotary tool for wrapping the coil

To better illustrate some of the main difference between different versions of the gripper, key attributes are summarized in Table 1.

Table 1: Comparing different versions of the gripper at a glance

	V1	V2	V3	V4	V5	V6
Coil Inner Radius, mm	25.4	25.4	25.4	18.67	23.25	21.25
Coil Outer Radius, mm	41.3	41.3	41.3	30.16	35	38.5
Coil Length, mm	29.5	59	59	78.87	35	39
Coil Wire Diameter, mm	0.64	0.64	0.64	0.51	0.64	0.64
Magnetic Shaft Length, mm	50.8	50.8	50.8	50.8	38.1	38.1
Magnetic Shaft Radius, mm	12.7	12.7	12.7	12.7	19.05	19.05
Gripper Overall Diameter, mm	94	83	85	80	100	100
Gripper overall Length, mm	125	136	155	205	124	120
Membrane Material	Latex	Latex	Latex	Latex	Silicone	Silicone
Membrane Type	Party Balloon	Party Balloon	Party Balloon	Party Balloon	Molded	Molded

Final version gripper's body was 11.7 cm long (without the shaft extended) and 11.5 cm wide in diameter which made it relatively small to attach it to most robotic arms. Gripper's length was designed to this length to keep it as short as possible, yet meet design criteria to have the maximum gripping force possible. This way it could easily be mounted on robots like Fanuc M-1*i*A series [75] to operate in small areas such as the area between two shelves. The overall gripper dimensions were chosen to keep it compact yet strong, capable of picking different range of objects. Gripper's simple design eliminated the need for any type of special sensors (except for a simple infrared and pressure sensor), and airlines for pumps like other conventional grippers. Therefore, it did not need a complex control algorithm to operate.

Sealed chamber inside the gripper was connected to a normally closed miniature solenoid actuated valve and a pressure sensor (NXP Semiconductors, MPX5010 series). This pressure sensor was not a critical component for this gripper. It was used to monitor the pressure inside the chamber to identify if the chamber seal was broken. It could also be used to regulate the pressure if sensitive objects were being handled and the membrane was applying excess force on that object.

There was only a single solenoid actuator (a coil and a shaft) used for this gripper's actuation. The use of solenoid made the gripping action much faster than other conventional grippers. The time it took the shaft to travel to the end of its stroke was 45

ms (the shaft traveled at 0.88 m/s when supplying 2.5 A current to the coil). The coil for this solenoid was specifically designed for this gripper with specific dimensions and specific wire gage which will be explained further in section 3.2. There were also an infrared emitter and an infrared receiver used to trigger the solenoid actuator based on the position of the shaft.

Permanent magnets were used instead of an iron core for this solenoid. The use of Neodymium magnets (NdFeB) increased the force this solenoid could generate and made it bidirectional, where you could change the solenoid into pull or push mode by simply swapping polarities of the coil. The shaft was made from a combination of Neodymium magnets and a plastic part made of Acrylonitrile butadiene styrene (ABS) material. The plastic part connected and sealed the membrane on one end, and connected to the Neodymium magnet on the other end. The outer diameter of the magnetic part of the shaft was 38.1 mm (1.5” magnet) and the plastic part had an empty slot where you could fit a smaller 25.4 mm diameter magnet. This 25.4 mm magnet secured the ABS plastic part of the shaft to the main 38.1 mm diameter magnet part of the shaft. Majority of the shaft was made from a stack of six (1.5 inch diameter and 0.25 inch thick) magnets. This configuration can be seen in Figure 3.9.

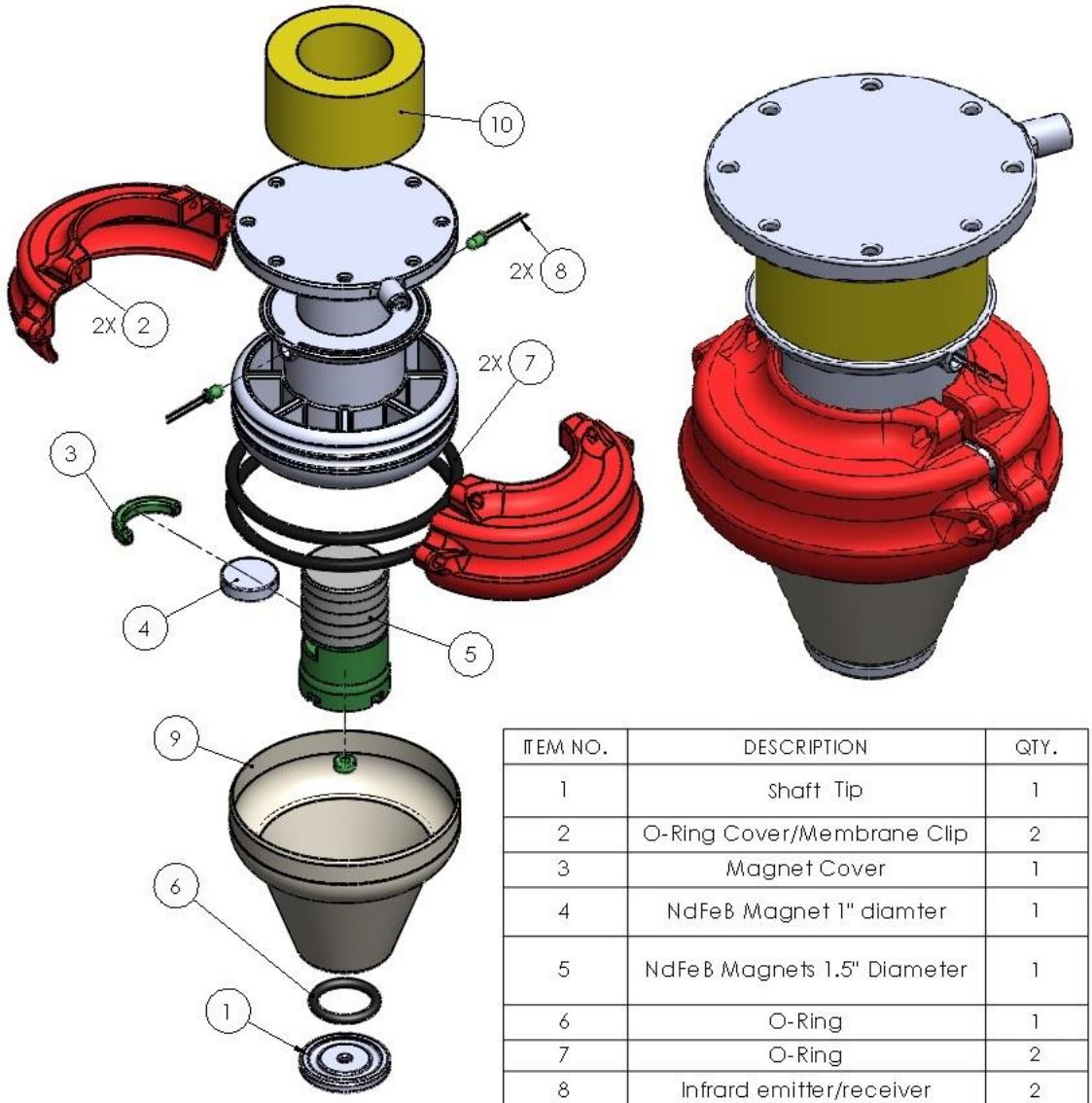

ITEM NO.	DESCRIPTION	QTY.
1	Shaft Tip	1
2	O-Ring Cover/Membrane Clip	2
3	Magnet Cover	1
4	NdFeB Magnet 1" diamter	1
5	NdFeB Magnets 1.5" Diameter	1
6	O-Ring	1
7	O-Ring	2
8	Infrard emitter/receiver	2
9	Flexible Membrane	1
10	Coil	1

Figure 3.9: Exploded and isometric view of the gripper in SolidWorks

In this design, the shaft was suspended in the middle of the gripper's chamber and it was supported by the membrane. In other words, the shaft was isolated from the gripper's main body. This gripper had only one flexible membrane and it was made of silicone from Smooth-on company [76]. This thin membrane sealed the main body of the gripper to the shaft, and its simple installation took less than one minute. Installation of the membrane needed 2 O-rings (9.5 cm inside diameter (ID) x 10.5 cm outside diameter (OD) each) to seal one end of this membrane to the gripper's body as shown in Figure 3.9. The other end of membrane was sealed to the shaft. Plastic part of the shaft had a groove to

put a small O-ring (3.4 cm ID and 4.2 cm OD) to seal the membrane to the shaft. There was another flat plastic part on the tip of the shaft that squeezed this O-ring with the membrane for a tight seal. The shaft and the membrane connection is shown in Figure 3.10.

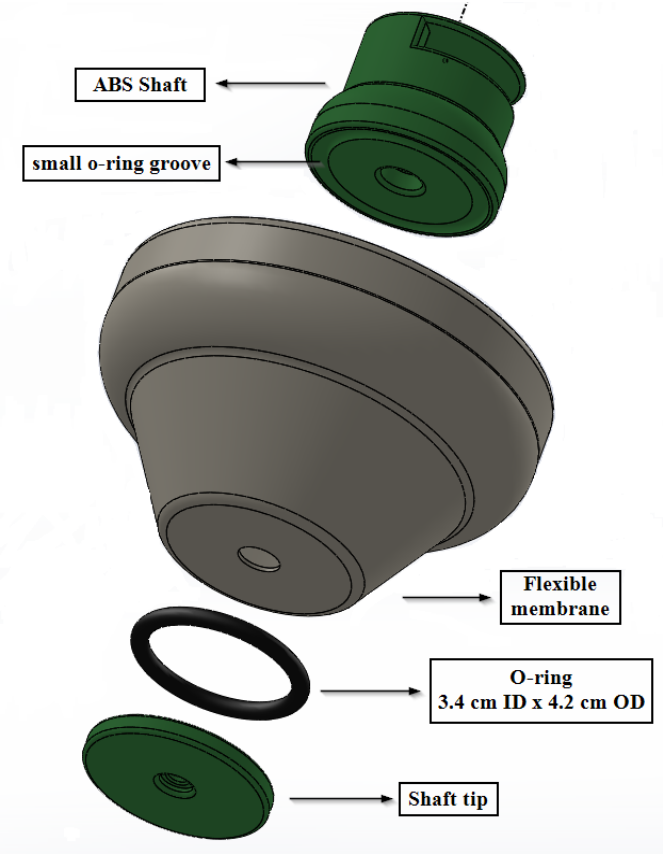

Figure 3.10: Sealing Membrane to the shaft

All plastic parts of this gripper that were designed in SolidWorks were 3-D printed using ABS plastic. ABS plastic can be dissolved using acetone. These parts were then exposed to cold acetone vapor for a better surface finish. The acetone vapor not only smoothened the surface of 3-D printed parts, but also caused the gripper's chamber to be sealed which was critical for operation of the gripper. The process of acetone smoothing ABS parts involved putting parts in a sealed container with acetone. The key point was that the acetone could not contact ABS parts directly, we only intended to expose the parts to acetone vapor. Acetone vapor then slowly dissolved ABS parts and made them much smoother. But one thing to note is that acetone vapor keeps reacting with ABS even after it is removed from the container. In other words, acetone vapor is soaked into ABS parts and keeps reacting until it is completely evaporated. Therefore, ABS parts needed to be

removed about half an hour before they reached the desired surface finish. Figure 3.11 shows a part which was exposed to acetone vapor for a long time and it was deformed. To better seal the chamber, all parts were then sprayed with clear coat spray. This spray also contained acetone which further sealed ABS parts surface.

Figure 3.11: Overexposure of an ABS part to acetone vapor

There are different 3D printing methods in the industry. Three major commercially available methods are Fused Deposition Modeling (FDM), Stereolithography (SLA), and Selective Laser Sintering (SLS). All prototypes have been made using FDM using ABS plastic. Hence, I could use acetone to smoothen their surface and achieve a better seal inside the gripper's chamber. ABSplus-P430 material was used in the FDM machine to print these prototypes, but it had 2 major problems. One was that it could not achieve a really good chamber seal even after acetone smoothing, and the other problem was its low heat deflection rate. If the gripper was used for prolong hours, the coil could potentially heat up. As a result, it could potentially deform the gripper's body since it was directly in contact with the ABS part. Hence, version 6 was also printed using SLA and SLS printers. Material used in SLS printing had a high heat deflection rate, but unfortunately its surface finish was really rough and it was much more porous than FDM printing. A high temperature resin was subsequently used in an SLA printer, which was developed by Fomrlabs [77]. It had a relatively high heat deflection rate after post curing the part with UV light and then thermally post curing it in an oven. It also had the best surface finish and printing accuracy in compare to the other two materials used in other printing methods. Table 2 shows the comparison of important properties used in all three printing methods.

Table 2: Different 3D printing methods and their respective material data

3D printing Method	3D Printing Material	Ultimate Tensile Strength	Heat Deflection Temp @ 1.8 MPa
FDM	ABSplus-P430	33 MPa	82 °C
SLS	PA11-GF3450	33 MPa	133 °C
SLA	FormLab High Temp Resin (post-cured)	526%	101 °C

To do a gripping task using a robotic arm, the gripper was connected to a KUKA robot (LBR iiwa 14 R820 [78]). In the gripping process, KUKA pushes the gripper and consequently its shaft toward the object being picked, and then the coil gets activated and the gripper grasps the object. KUKA arm approaches the object being picked, during which the coil is off and the solenoid valve is open. Then KUKA lowers the gripper over the object. Right before lowering the gripper, solenoid valve closes and seals the chamber (Figure 3.12-A). Tip of the suspended shaft hits the object (Figure 3.12-B) , and it starts to be pushed further inside the chamber as KUKA lowers the gripper further down over the object. As a result of this action, the volume difference in chamber causes a positive pressure, which results in the membrane getting inflated. This inflation in membrane causes it to become like a toroid and form itself around the object (Figure 3.12-C). Surface area between the membrane and the object is increased as the gripper gets closer to the object. Friction between the membrane and the object helps with grasping the object. This formation of the membrane also creates a sealed pocket between the object and the shaft of the gripper. Gripper's infrared sensor activates the coil as soon as one end of the shaft blocks its emitter path. KUKA only lowers the gripper until the point where infrared sensor is triggered (Figure 3.12-C). Right before the coil is activated, object has reached the closest point to the gripper, and gripper's body is against the object. When the coil gets activated, the shaft is pulled all the way to top of the chamber. This further increases the positive pressure inside the chamber which creates a stronger normal force applied on the object where it is contacting the membrane. Therefore, the friction between the membrane and the object is increased. Due to the object being held stationary and the shaft moving further up, volume difference between the shaft and the object causes a strong negative pressure which creates a strong suction to hold the object like vacuum suction grippers. Then KUKA moves the object to desired location (Figure 3.12-D) and releases it by deactivation the coil. Right after the coil is deactivated, the solenoid valve opens and

changes the pressure inside chamber to normal which is the atmospheric pressure. This pressure release inside the chamber also helps with releasing the object being picked.

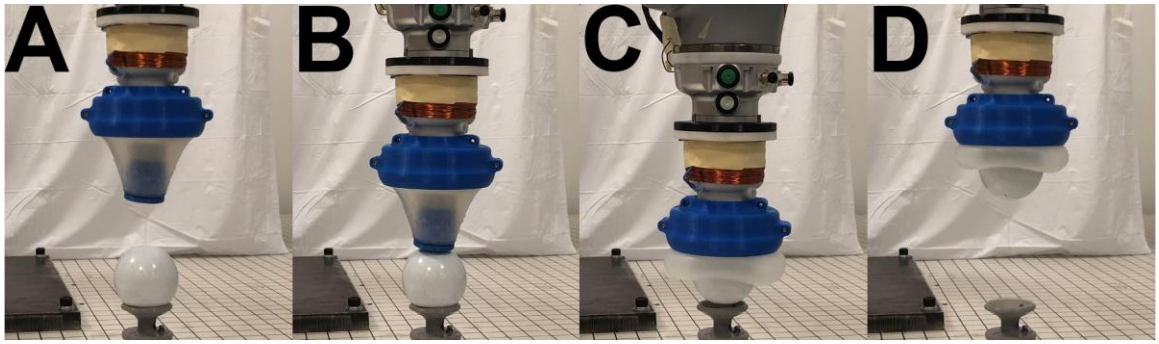

Figure 3.12: Pictures of different stages of gripping an object

3.2. Gripper actuation

3.2.1. Solenoid Actuation

To achieve and maintain a strong actuation force with high speed, a solenoid actuator was developed and implemented for the gripper. The main components of the solenoid are a coil and a ferromagnetic shaft that is free to move inside the solenoid. The coil is a long wire wrapped around a tube called bobbin in form of a tightly packed helix. When current is passed through the coil, it generates a magnetic field, and its direction depends on the direction of current in coil. Hence the coil in the solenoid becomes an electromagnet. Magnetic field generated by this electromagnet moves the ferromagnetic shaft in solenoid. Strength of this electromagnet can be adjusted by changing the current in wire.

Most solenoid actuators have a metal shaft in the middle and a spring behind this shaft. In such actuators, the magnetic field attracts the shaft to the center of the solenoid core, and a spring pushes it out to the normal position after electromagnet is turned off. In contrast, the solenoid design proposed here incorporates a permanent magnet as a shaft to further increase the actuation force of this solenoid. In this case, the solenoid force becomes a combination of the electromagnetic force created by the coil, as well as the magnetic force generated by the permanent magnet. The permanent magnet has a fixed north and south poles, but polarity of the electromagnet could be changed by changing polarity of the current going through the coil's wire. Therefore, another advantage of using permanent magnet in the solenoid actuator was that it could push and pull the shaft by

simply changing the direction of current in the solenoid's coil. In order to further increase the actuation force of the solenoid, neodymium magnets (NdFeB), which are a type of rare earth magnets were used. These magnets were the strongest type of magnets available in the market. Figure 3.13 shows the proposed solenoid with a permanent magnet shaft.

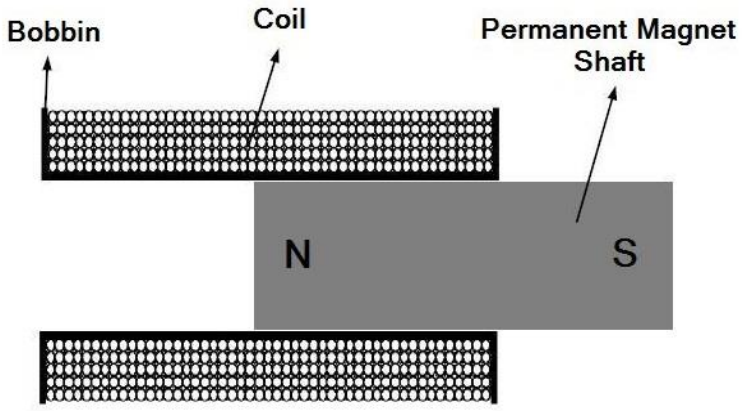

Figure 3.13: Cross Section of a solenoid made of a coil and a permanent magnet shaft

A test setup was made to measure electro magnetization force on different types of shafts in a solenoid. A commercially available premade coil was purchased [74], and different types of shafts were used. A luggage scale was used as the force sensor. This sensor was fixed to a leveling device fixed to a table which could be adjusted up and down. Figure 3.14 shows this setup. Please note the coil and magnet are not shown in this figure as they are changed during each test. The coil was fixed to the table and the shaft was attached to the force sensor suspended over the coil. After coil was activated, shaft was slowly lowered and its displacement with respect to the coil and the force sensor's reading was recorded.

Figure 3.14: Force sensor attached to a leveling device

The purchased coil including its bobbin had 37.33 mm inside diameter, 60.33 mm outside diameter, 52.58 mm length, and 1574 coil turns. In order to better compare the actuation force on different shafts, a 24 V voltage was applied to the coil, with 1.14 A current and it was kept constant during the whole test. Three different shafts were used which had identical lengths and outside diameter. Figure 3.15 shows the comparison between these shafts and it clearly proves that the actuation force of a solenoid using a permanent magnet as a shaft is more than using a metal shaft. Also the solid fill cylindrical magnet shows a higher force than the hollow magnet due to the higher magnetic force. Displacement shown in Figure 3.15 is the displacement between center of the coil to center of the shaft. Force measurement was done by attaching the shaft to a force sensor.

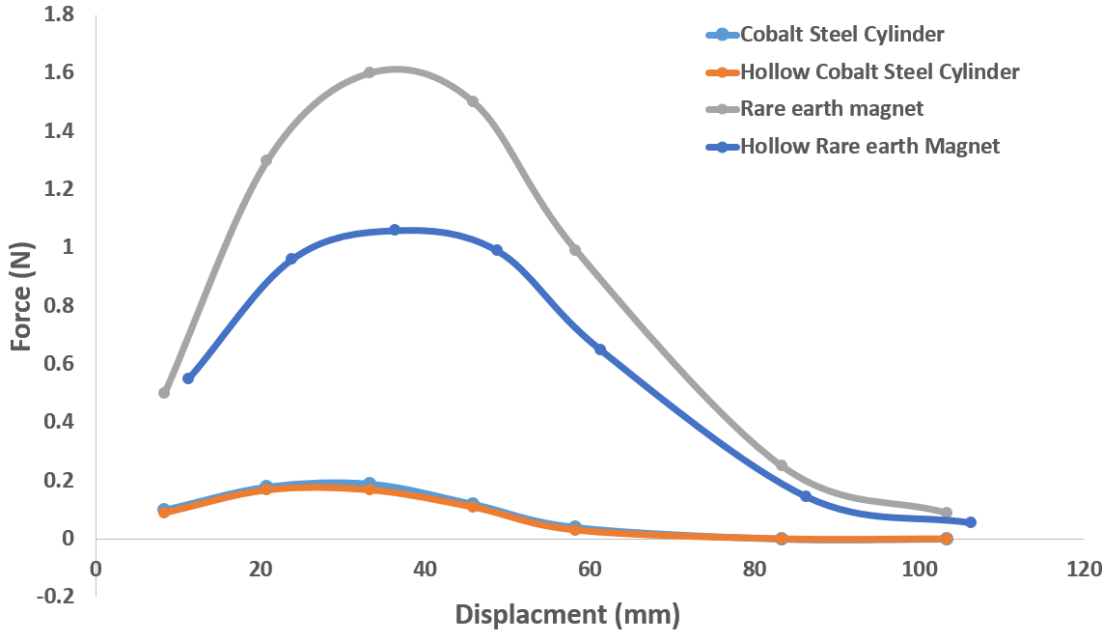

Figure 3.15: Shaft comparison between a solid fill cobalt steel cylinder, a hollow cobalt steel cylinder with 21 mm inside diameter, a solid fill rare earth magnet, and a hollow rare earth magnet with 12.7 mm inside diameter

To better understand the shape of the curve in Figure 3.15, we will further examine behavior of the permanent magnet shaft when exposed to the magnetic field generated by a coil. Permanent magnet shaft has a fixed north and south pole, but polarity of the coil can be changed by changing polarity of the current applied. Please note that the polarity of a coil is mainly determined based on the direction of wire wrapped around the bobbin, and then it will be determined using right hand rule base on direction of the current applied. Depending on polarity of the coil, it will either pull or push the magnet. As show in Figure 3.16, permanent magnet shaft will be attracted toward the coil if its polarity and coil's polarity are in opposite direction, but it will be repelled away from the coil if their polarities have the same direction.

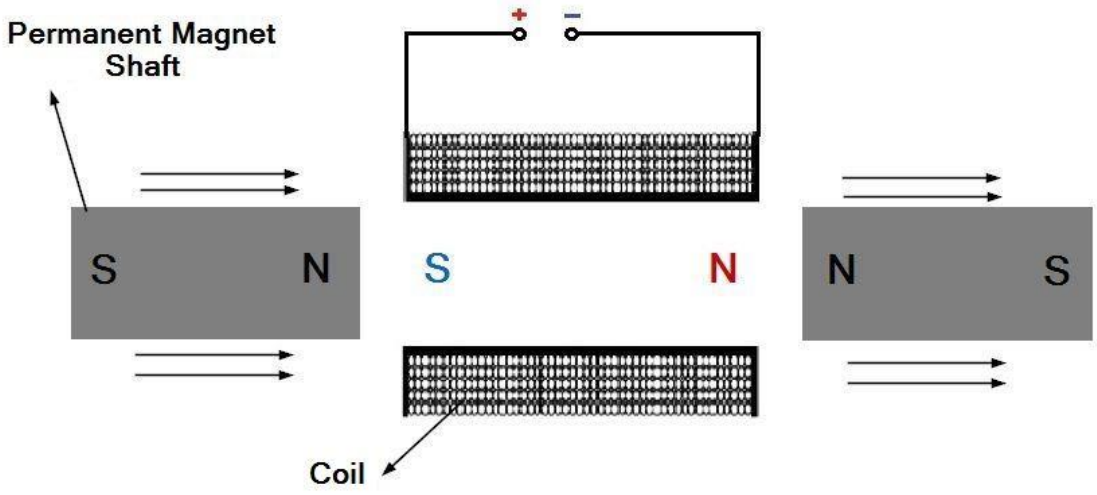

Figure 3.16: Cross section of an energized coil and a set of permanent magnet shafts

Since both the shaft and the coil are magnetized, they will have an equilibrium point where shaft stays still in the coil. In other words, if the coil is pulling the magnetic shaft inside its core, it will pull until the magnetic shaft reached this equilibrium point. This equilibrium point is where the center point on the coil aligns over the center point of the magnetic shaft. Figure 3.17 better illustrates this point. Both magnets in this figure are in a neutral position and they will not move neither to the left nor to the right of the coil.

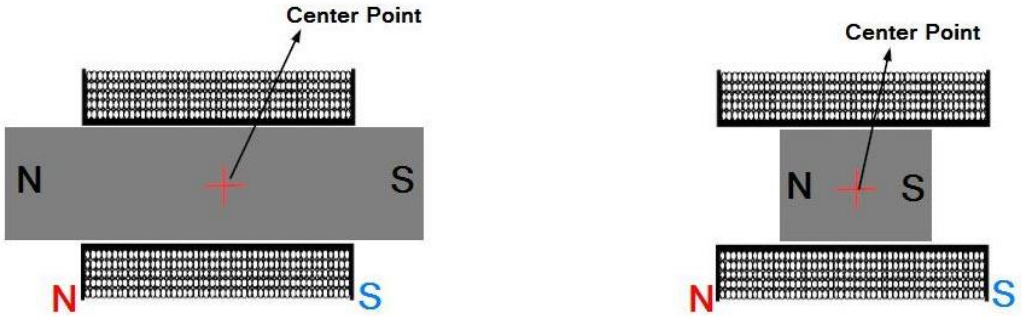

Figure 3.17: Cross section of a pair of identical coils with two different size magnets

Actuation force greatly depends on the distance of the permanent magnet shaft to the coil. As the permanent magnet shaft's length gets longer, its magnetic field increases and as a result the actuation force increases. Also the longer the shaft, the more it can travel until it reaches the equilibrium point shown in Figure 3.17. Let's consider the case where we have a permanent magnet shaft that is longer in length than the coil. Actuation force gets stronger as the magnetic shaft's center point gets closer to coil's center point,

but it starts to decline as the edge of the magnetic shaft passes the center point in the coil. Please note that the force distribution graph shown in Figure 3.18 is only for illustration and the points on the curve are just an estimated displacement between the coil and the shaft.

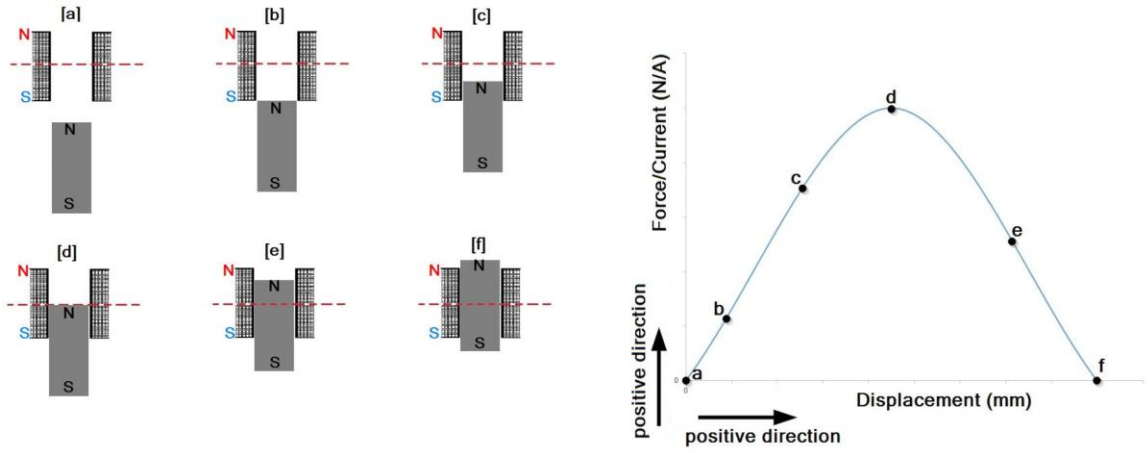

Figure 3.18: Actuation force with respect to displacement of the magnetic shaft to the coil

3.2.2. Coil Experimental Investigation

The only actuator used in the gripper was a solenoid actuator which had a permanent magnet as the shaft. Solenoid actuator comprised of a wire wrapped around the solenoid structure, and a permanent magnet shaft movable in the middle of a coil. Neodymium magnets were used as the shaft material to enhance the net force of solenoid and allow the shaft movement to be bidirectional. Once a voltage was applied across the coil, its magnetization resulted in pushing or pulling of the magnetic shaft based on the polarity of the coil. Parameters of the coil and magnet should be carefully designed to achieve a desired force within the solenoid.

To better understand the force created by using different coils and different permanent magnets, several tests were implemented and measurements were done. A setup like the one in section 3.2.1 was made, where the coil was fixed to a table and the magnetic shaft was attached to a force sensor. Most of these tests were done using over the counter coils that were purchased from APW Company [74] unless otherwise noted. From the test in section 3.2.1, we learned that using a permanent magnet shaft created

the maximum actuation force. Hence in the next few tests we only used permanent magnet shafts.

The following test is showing the difference between using one coil vs two coils. All parameters were kept constant, except length of coil that was doubled. The coil used in this test had product number FC-4840. Each coil had 50.8 mm inside diameter, 82.6 mm outside diameter, 29.5 mm length, and 345 number of turns. The same shaft was used for both setups and it had 25.4 mm diameter and 50.8 mm length. The first test used only one FC-4840 coil and the second test had two FC-4840 coils in series with each other forming as one single coil with double length or number of turns. Therefore, we had to double up the voltage in the second test to get the same current rating. Figure 3.19 indicates that longer coil had stronger actuation force.

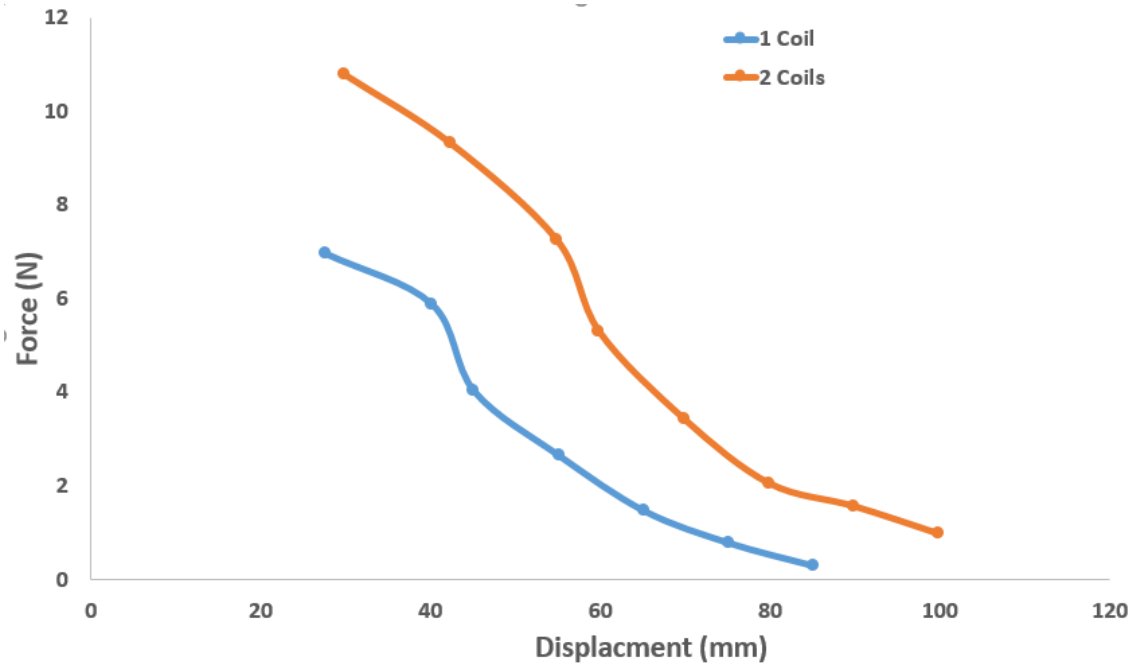

Figure 3.19: Comparing actuation force when doubling coil length and keeping everything else constant

In the following graph shown in Figure 3.20, we were comparing the force between two shafts with different diameters. Both shafts were permanent magnets with 38.1 mm length, but one shaft had 25.4 mm diameter and the other one had 38.1 mm diameter. The coil used in this test was FC-4839 and it had 50.8 mm inside diameter, 82.55 mm outside diameter, 29.47 mm length, and 680 number of turns. Figure 3.20 shows that using a magnetic shaft with a bigger diameter effectively increased the actuation force.

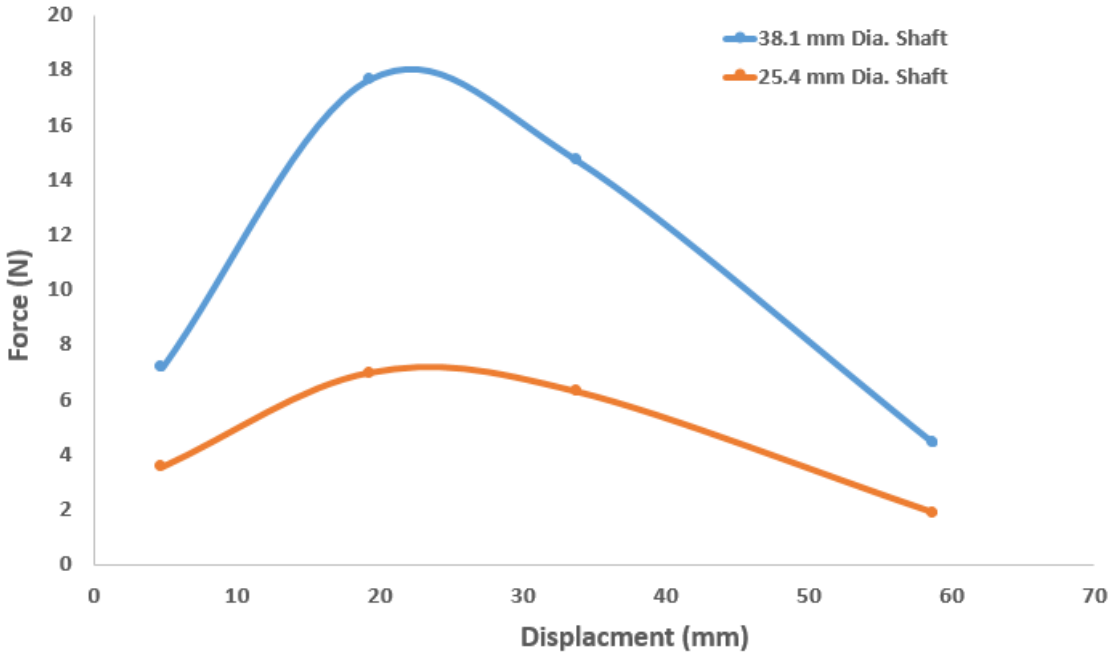

Figure 3.20: Comparing actuation force when two shafts with different diameters are used and all other parameters are kept constant

In the following test, actuation force was compared between two magnetic shafts with different lengths. All other dimensions and parameters were kept constant. One magnetic shaft was 88.9 mm long, and the other permanent magnet shaft was 31.75 mm long. The coil used in this test was a combination of two coils (FC_6271) in series. Considering both coils as one, the coil had 52.58 mm length, 60.33 mm inner diameter, 37.34 mm outer diameter, and 787 number of turns. Figure 3.21 shows this comparison.

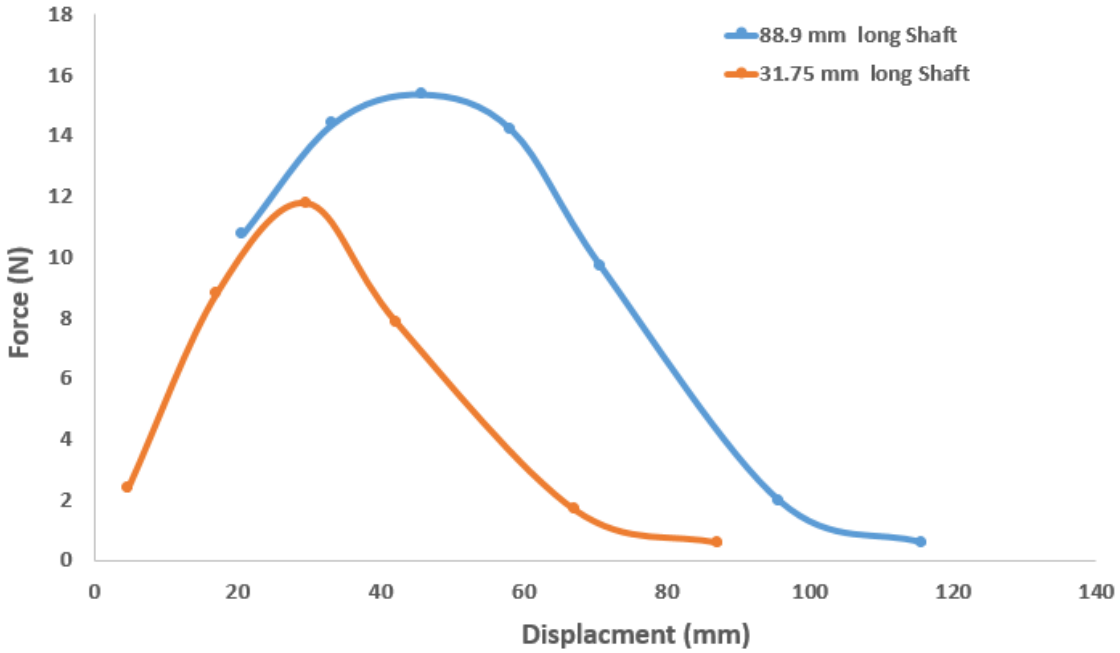

Figure 3.21: Comparing actuation force when two shafts with different lengths are used and all other parameters are kept constant

Another test was done to compare actuation force when we used coils with different lengths. In this test the magnetic shaft was 25.4 mm wide and 88.9 mm long. One coil was 78.88 mm long and the other coil was 52.58 mm long. The shorter coil was a combination of two coils in series (FC-6271) and the longer coil was three coils (FC-62.71) connected to each other in series. In order to keep the current comparable, shorter coil was set to 24V which drew about 1.14 amp current and the longer coil was supplied with 36V power to draw about the same amount of current as the shorter one. Figure 3.22 better illustrates this comparison.

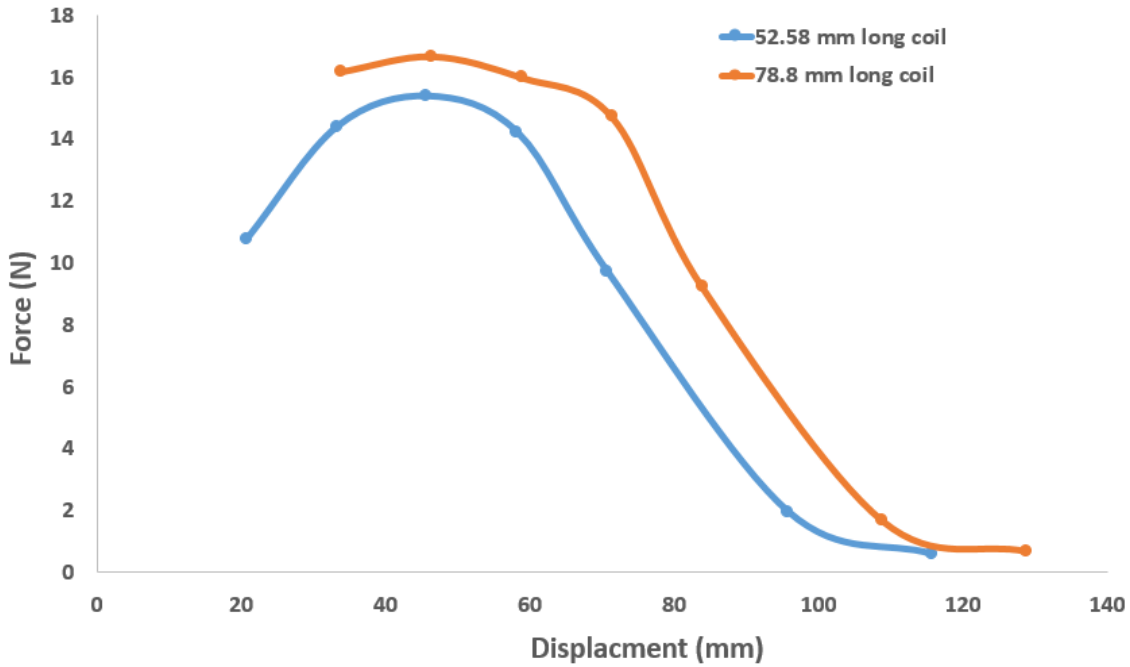

Figure 3.22: Comparing actuation force when two coils with different lengths are used and all other parameters are kept constant

Knowing solenoid can be a feasible solution for this gripper, I decided to make my own custom coils. On this next test, I made three coils and tested them using an identical shaft. In other words, these coils were not bought from a store and were wrapped manually. Three identical coil bobbins with 46.5 mm inside diameter, 70 mm outside diameter and 35 mm length were 3D printed using ABS plastic. A bobbin holder was 3D printed and attached to a drill and three different coils were wrapped manually. The first coil was wrapped using 20 AWG (0.8128 mm diameter) wire [79], the second coil was wrapped using 22 AWG (0.6452 mm diameter) wire [79] and the third coil was wrapped using 24 AWG (0.5105 mm diameter) wire [79]. The shaft used in this test had 38.1 mm diameter and 38.1 mm length. In this following test we set some constraints to better compare these coils. The maximum voltage and current allowed was 24 V and 3 A respectively. In other words, we increased the voltage until either the voltage or the current reached the maximum allowed. All other parameters of the coils and permanent magnet shafts were kept constant, except the wire gauge each coil was wrapped with. The shaft had 38.1 mm diameter and 38.1 mm length. Figure 3.23 shows the comparison between these three coils. The 20 AWG coil was running at 10 V and 2.94 A, the 22 AWG coils was running at 24 V and 2.96 A, and the 24 AWG coil was running at 24 V and 1.23 A. Please note that after testing custom coils, they can be requested to be made if they are superior over other coils. They can be ordered to be made from companies like APW [74].

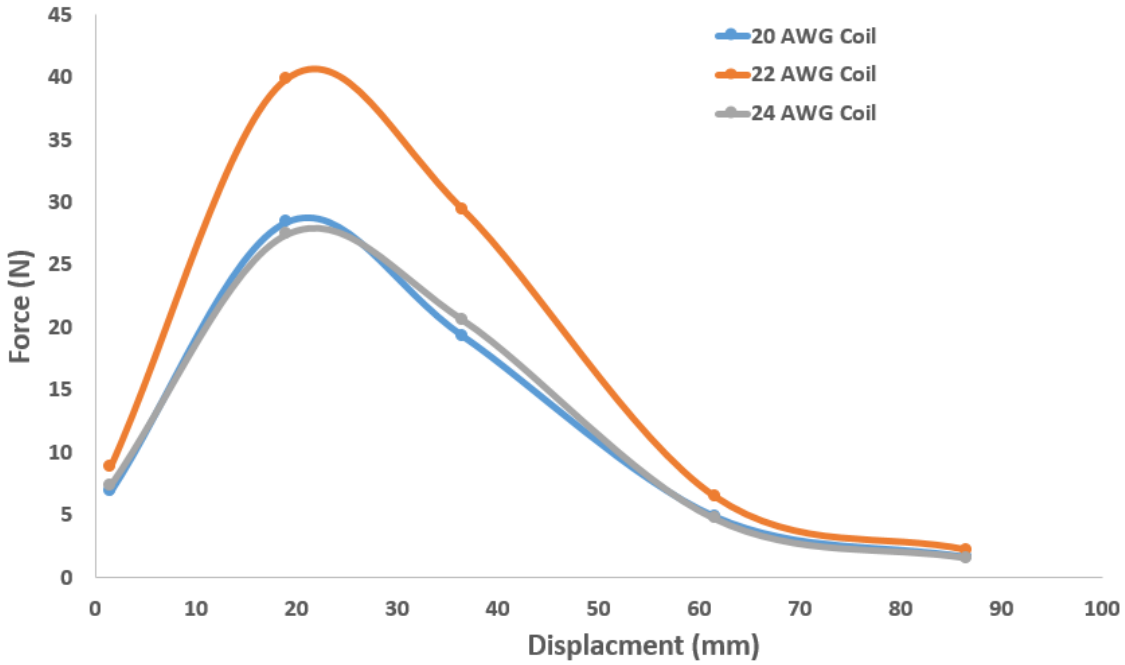

Figure 3.23: Comparing three custom wrapped coils using different wire gauges

3.2.3. Solenoid Model

In general, the force between a cylindrical coil and a magnetic shaft is a function of the main geometrical parameters of the coil and the magnet. The main geometrical parameters of the coil and the magnetic shaft actuator are shown in Figure 3.24 (modified from [80]) and are defined as follows. As defined by Robertson et al. [80], R_m and l_m represent the magnet's radius and length, r_c, R_c are coil's inner and outer radius, l_c is the coil's length, N_r and N_z are the number of coil turns in the radial and axial directions, and z represents the center to center distance between the magnet and the coil.

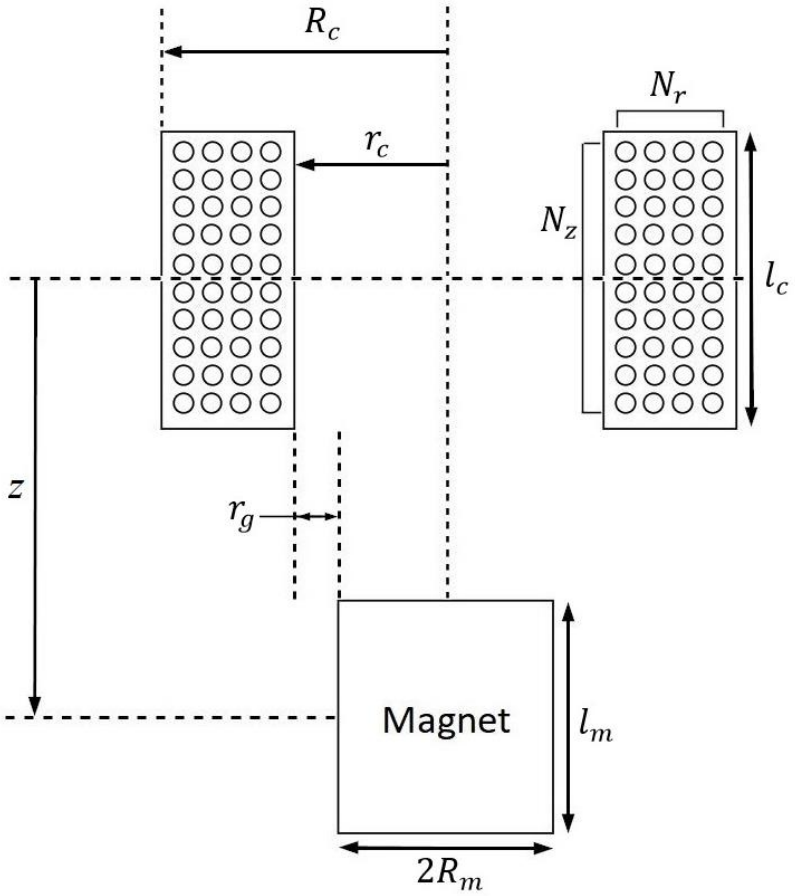

Figure 3.24: Geometrical parameters of the coil and magnet actuator (modified from [80])

The push or pull force applied to the permanent magnet (shaft) by the energized thick coil is calculated using the following equation, which is the summation of forces created by N_r number of thin coils separated in radial direction [80], [81]:

$$F_z = \frac{1}{N_r}\sum_{n_r=1}^{N_r} F_s(R_m, r(n_r), l_m, l_c, z) \tag{2}$$

$$r(n_r) = r_c + \frac{n_r - 1}{N_r - 1}[R_c - r_c] \tag{3}$$

where F_s is the axial force between the magnet and a thin coil with length l_c. F_s is given by:

$$F_s(R_m, r, l_m, l_c, z) = \frac{J_1 J_2}{2\mu_0}\sum_{e_1,e_2}^{\{1,-1\}^2} e_1 e_2 m_1 m_2 m_3 f_s \tag{4}$$

where $J_1 = B_r$ is the magnetization of the magnet, $J_2 = \frac{\mu_0 N_z I}{l_c}$ is the magnetization of the coil with a current I going through the coil's wire, and $\mu_0 = 4\pi \times 10^{-7}\ {}^{N}/_{A^2}$ is the magnetic constant. The term f_s in (4) is given by:

$$f_s = K(m_4) - \frac{1}{m_2}E(m_4) + \left[\frac{m_1^2}{m_3^2} - 1\right]\prod\left(\frac{m_4}{1-m_2}\middle| m_4\right) \tag{5}$$

with parameters:

$$m_1 = z - \frac{1}{2}e_1 l_m - \frac{1}{2}e_2 l_c,$$

$$m_2 = \frac{[R_m - r]^2}{m_1^2} + 1,$$

$$m_3 = \sqrt{[R_m + r]^2 + m_1^2},$$

$$m_4 = \frac{4R_m r}{m_3}. \tag{6}$$

The functions $E(m)$, $K(m)$, and $\prod(n|m)$ are the complete elliptic integrals of the first, second, and third kind respectively with parameter m.

3.2.4. Solenoid Model Verification

Equations (2)-(6) were used to simulate the push, pull force applied to the magnet of the proposed gripper. These analytical equations were implemented in Matlab by adapting and modifying a publicly available code at a GitHub repository [82]. To ensure the validity of the presented constitutive equations for the proposed gripper configuration, a series of experiments were performed for the prototyped gripper and the measurements were compared with the simulated results. The experimental results were recorded by doing a test like the one mention is section 3.2.1, except the prototype gripper was fixed to the table upside down instead of just a commercially purchased coil.

The objective of the experiments was to measure the amount of force applied to the shaft by the fixed coil. The gripper structure was vertically fixed to the table in an upside-down position and the coil was energized with a certain current. The neodymium shaft, which was coupled to a force sensor, was slowly lowered toward the center of the coil while the force sensor readouts and the shaft to coil distance were recorded. The readouts represented the coil pull force on the shaft for variable distances. Table 3 shows the parameters used in the prototyped coil and magnet actuator.

Table 3: Prototyped coil and magnet actuator

Parameter	Value
Coil length	39 mm
Coil OD	77 mm
Coil ID	42.5 mm
Coil radial turns	26 turn
Coil axial turns	61 turns
Magnet diameter	38.1 mm
Magnet length	38.1 mm
Magnet magnetization	1.1 T

Figure 3.25 shows the amount of force for different distances in both experimental measurements and the analytical calculations. Figure 3.25 shows that the error between the analytical calculations and experimental measurements are less than 5% and the analytical simulations could be used to explore the design parameters of the solenoid.

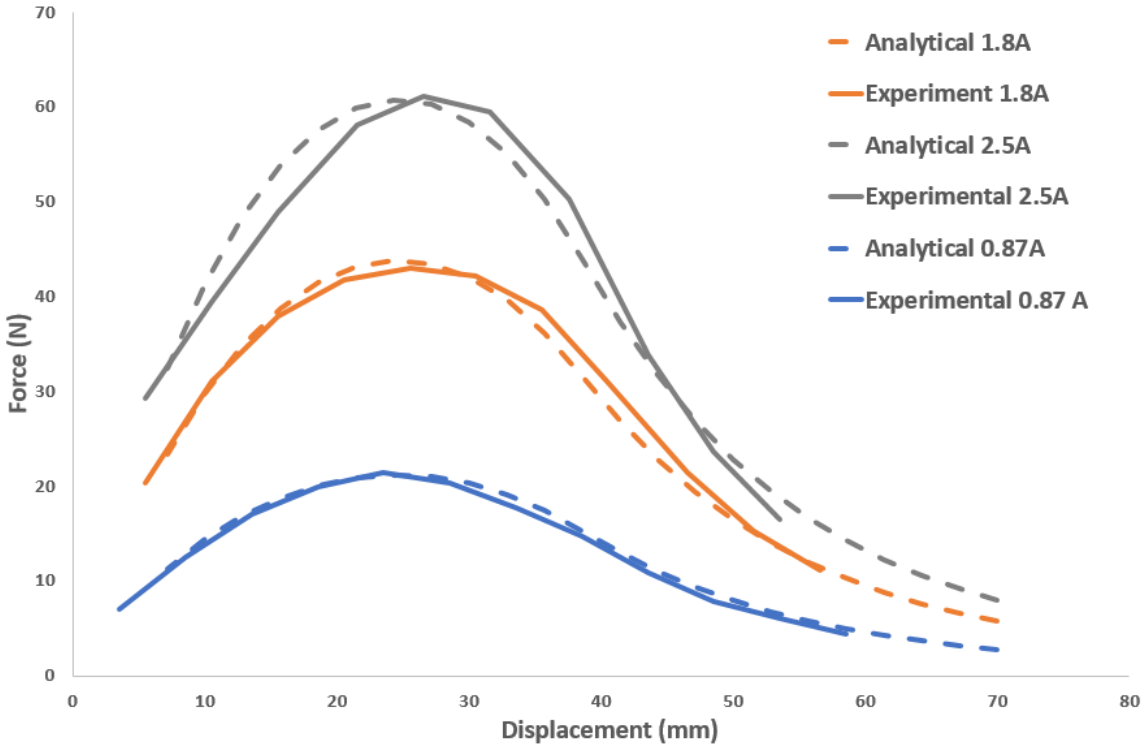

Figure 3.25: Comparison of analytical and measured force values using the designed gripper

3.2.5. Solenoid Design Consideration

Given the close match between analytical and experimental results, the model was then used to draw considerations about the design of the gripper. In order to obtain desirable gripper parameters, two parameters were defined to better characterize the design: coil ratio, α defined as the coil length over the coil inner radius and Magnet ratio β defined as the magnet length over magnet radius.

$$\alpha = \frac{l_c}{r_c} \tag{7}$$

$$\beta = \frac{l_m}{R_m} \tag{8}$$

R_m is the radius of magnet and r_c could be obtained by using equation (9) and considering a gap r_g between the magnet and the coil:

$$r_c = R_m + r_g. \tag{9}$$

Ideally, r_g should be zero to maximize the coil generated magnetic field area, which is interacting with the magnetic shaft. However, in real case scenario, the coil is wrapped around a support surface causing a non-zero r_g. Knowing R_m, the magnet length l_m could also be obtained using the design parameter β.

For the proposed gripper, r_c could be determined based on the radius of the magnet R_m, used as shaft. Thus, providing r_c is a given geometrical parameter, the coil length l_c could be obtained using the design parameter α.

By assuming that the thickness of the wire insulation is negligible, R_c could be calculated using the following equation [80]:

$$R_c = \sqrt{{r_c}^2 + \frac{l_w {d_w}^2}{\pi l_c}}; \tag{10}$$

where d_w is the coil's wire diameter. The wire length l_w could be calculated from the following formula:

$$l_w = \frac{R \cdot \alpha_w}{\rho} \tag{11}$$

$$\alpha_w = \pi \left[\frac{d_w}{2}\right]^2 \tag{12}$$

where R is the coil's wire resistance, α_w is the coil's wire cross sectional area, and ρ is the resistivity of coil's wire.

The coil turns N_r and N_z, could be obtained from the following equations:

$$N_r = (R_c - r_c)/d_w, \text{ and} \quad (13)$$

$$N_z = l_c/d_w. \quad (14)$$

Using equation (2) and applying coil turns N_r and N_z, and various arbitrary values for coil and magnet ratios, α and β, as inputs, the coil actuator force per input current versus distance curves could be calculated. The obtained curves could provide valuable design insights for the gripper. As an illustrative example, using the parameters from the prototyped gripper of this paper, Figure 3.26 and Figure 3.27 show the coil and magnet force per current versus distance for various design parameters α and β respectively. Please note that each figure has three sets of curves based on three values for magnet radius R_m *= 1", 1.5", and 2"*.

The following values were used or selected for the prototyped gripper. The maximum operating voltage for the coil actuation was set to 36 V due to the limitation of the chosen power supply. Given the maximum power supply current of 2.5 A, the nominal wire resistance was considered to be $\frac{V}{I} = 14.4\ \Omega$. To make the coil, a copper wire with resistivity of $\rho = 1.7 \times 10^{-8}$ Ω.m and diameter d_w of 0.64mm (wire 22 AWG) was chosen. The selected wire safely allowed passage of 2.5 A current without damaging the insulation around the wire while allowing for a maximum number of coil turns. For the gripper prototype of this paper, a 1 mm wall thickness, which is the barrier between coil and chamber was considered. The wall thickness was chosen based on considering a reasonable minimum thickness to provide a reasonable mechanical support in the gripper's structure. A 0.5 mm air gap was also considered to provide a reasonable clearance for the magnetic shaft. Since the 3D printer resolution for printing the coil's wall thickness was 0.25 mm, the gap of 0.5 mm was suitable to ensure proper mobility of the magnetic shaft. Although the prototyped gripper had 1.5 inches magnetic shaft, the magnet radius was variable between three values, R_m *= 1", 1.5", and 2"* based on the commercially available rare earth cylindrical magnets. These range of values were chosen to search a wider range of radius for the magnet design. Smaller radius for the magnetic shafts would have caused a weak gripper, and bigger ones would have made the gripper

too big for common practical applications. The coil inner radius was defined by adding 1.5 mm to magnet radius. α and β values were chosen to be 1 and 2 respectively.

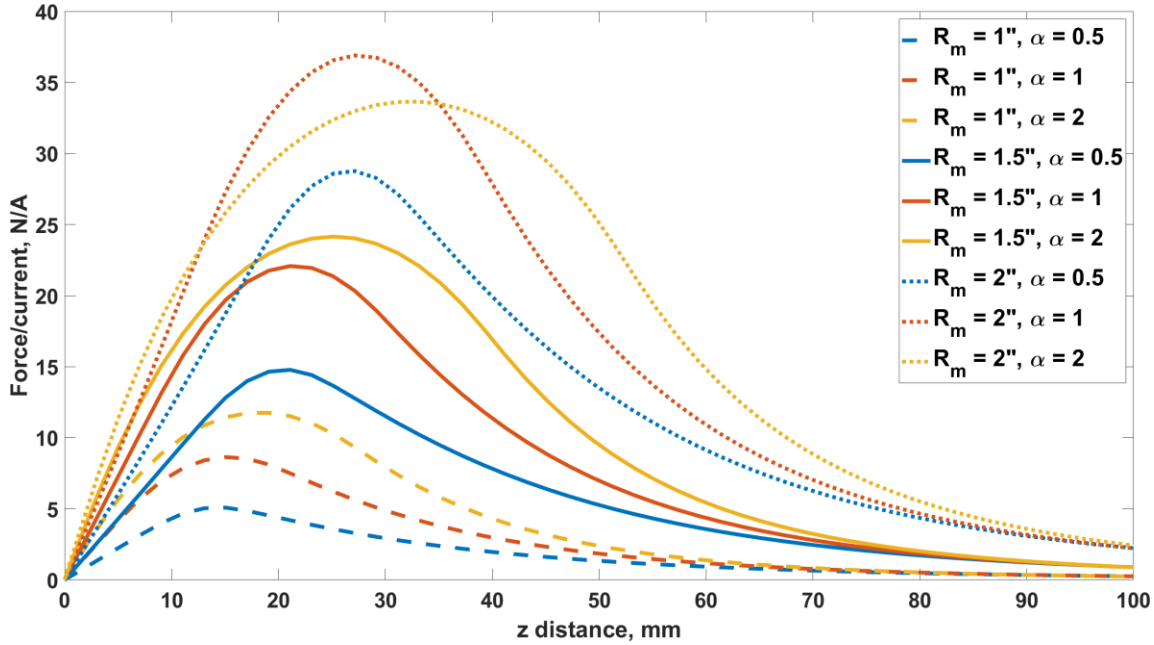

Figure 3.26: Normalized force vs center to center distance for different coil ratios

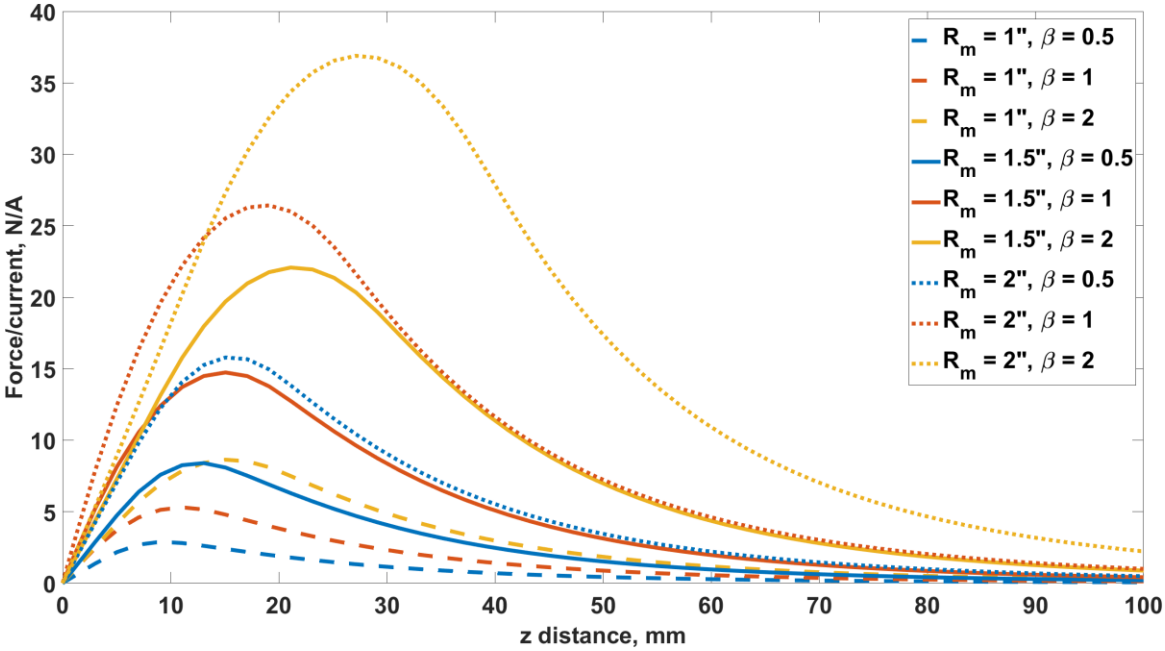

Figure 3.27: Normalized force vs center to center distance for different magnet ratios

Using the chosen parameters, the plots in Figure 3.26 and Figure 3.27 where generated. Referring to Figure 3.26 , the coil ratio α is varied while the magnet ratio β is kept constant at β = 2. As α is increased, the distance z at which the maximum normalized force is achieved is also increased which means that a larger travel distance is required for the magnetic shaft to reach a maximum force. Within the chosen range of variation for α in Figure 3.26, α = 1 provided the maximum force for a 1.5 inches magnet as shaft.

Referring to Figure 3.27, the magnet ratio β is varied while the coil ratio α is kept constant at α = 1. As β is increased, the distance z at which the maximum normalized force is achieved is also increased which means that a larger travel distance is required for the magnetic shaft to reach a maximum force. Within the chosen range of variation for β in Figure 3.27, as beta increased, the maximum force generated by the solenoid actuator was also increased.

The sensitivity of the force function based on α and β was shown in Figure 3.26, and Figure 3.27. An optimization algorithm can be used to obtain optimum α and β values for a solenoid actuator design. An arbitrary initial constant α and β could be chosen to obtain optimum value for the force applied to a magnetic shaft by a thick coil.

3.2.6. Solenoid Optimization

Three different global optimization algorithms extensively used in the literature were compared to obtain the optimum results for a gripper with a coil and a magnet. Genetic Algorithm (GA), Simulated Annealing (SA), and Pattern Search (PS) were the global optimization algorithms used to obtain the minimum optimum point. The optimization function, constants and variables were defined. Most important factor in using global optimization algorithms is to converge to a solution [83], and converging to an optimum solution is significantly defined by choosing the right optimization function and parameters that are passed to this function [84]. Then the performance and results of mentioned optimization algorithms were compared to find the best suitable result.

Genetic Algorithm adopts a search algorithm based on a natural biological evolution [85]. A randomized population sample is first chosen and then according to Darwin's theory "survival of the fittest" [84], the weaker individuals are eliminated and the fitter individuals are chosen to create the new population by using genetic operators like crossover and mutation. GA only needs function values and gradients is not required.

Simulated Annealing was originally inspired by the physical annealing process. In the process of accepting new function values to find the optimum result. SA not only accepts point with smaller function value for new iteration, but it also accepts some point with a bigger function value [86]. The rate of acceptance for new points gets smaller, similar to the temperature decrease in the physical annealing process [87]. Therefore, it does not get stuck in local minimums, and it is suitable to find the global optimum.

Pattern Search, similar to GA, does not require gradient information. PS is an exploratory search where it compares two function values and finds its direction. It takes large step sizes to find the next point to evaluate. As soon as there is no improvement in the function value of next point, PS keeps reducing the step size in finding the next point until the improvement in function value is sufficiently small [88], [89].

Equation (2), is the force applied to the permanent magnet by the coil of the gripper. Our goal was to find the optimum point of this function which would be the maximum force applied. All the mentioned global optimization algorithms are designed to find the optimal minimum of a function. Therefore, the output value of the force function in equation (2) needed to be multiplied by negative one. In order to calculate this force function, equations (7)-(14) were needed to determine characteristics of the coil and the permanent magnet. Variables of this optimization problem were α, β, and d_w. The wire gauge (d_w, wire diameter) was also added as another variable to this optimization problem since it is a significant element of the gripper's coil. In order to solve equations (7)-(14) and evaluate the force function, some constants had to be defined. Table 4 shows the constant parameters used in the proposed optimization problem.

Table 4: Constant parameters for the coil and magnet

Parameter	Value
Coil's wire resistivity, ρ	$1.7 \times 10^{-5}\ \Omega.mm$
Magnet magnetization, J	$1.1\ T$
Gap between magnet and coil, r_g	$1.5\ mm$
Coil's wire impedance, R	$14.4\ \Omega$
Magnet Volume, V_m	$4.35 \times 10^4\ mm^3$

Wire resistivity ρ was set to copper wire's resistivity since it is the most common used wire for coils. Magnetization J, is the magnetization of the neodymium magnets purchased. r_g is the gap between the coil and the magnetic shaft, which was set to be 1.5 mm. Similar to the explanation in section 3.2.5, this value of 1.5 mm was arbitrary selected based on the pragmatic consideration that the coil's bobbin thickness was considered a minimum of 1 mm and a 0.5 mm gap was added to allow the shaft freely slide up and down in the coil. In order to perform the optimization and converge to an optimized point, two optimization equality constraints had to be defined [80], namely coil impedance and magnet volume (shaft volume). In other words, designing an optimized magnetic solenoid for a gripper is narrowed down to choosing only the coil impedance and the magnet volume, and all other required parameters are implicitly derived based on these two chosen parameters. The coil impedance for this optimization was chosen based on the available power supply we had in the lab and it was therefor limited to 14.4 Ω. The magnet volume (shaft volume) was chosen to be the same of the prototyped gripper ($4.35 \times 10^4\ mm^3$). While a different volume could have been selected, this choice enabled me to identify the optimal parameters of α, β, and d_w which could be used to maximize the performance of the gripper developed in this thesis.

In order to derive the other parameters shown in equations (7)-(14), these formulas need to be rearranged. The magnetic shaft is a cylinder and its volume is:

$$V_m = \pi {R_m}^2 \cdot l_m \tag{15}$$

Therefore, R_m in terms of V_m, and l_m is:

$$R_m = \sqrt{\frac{V_m}{\pi \cdot l_m}} \tag{16}$$

Since one of the optimization variables is the coil ratio β, and other coil parameters need to be calculated based on the optimization variables, then equation (16) is plugged into equation (8) and solved for l_m:

$$l_m = \left(\beta \cdot \sqrt{\frac{V_m}{\pi}}\right)^{2/3} \tag{17}$$

Subsequently r_c can be derived from equation (9), and equation (7) can be written based on α and r_c:

$$l_c = \alpha \cdot r_c \tag{18}$$

Now using equations (9)-(14), all parameters are derived based on optimized α, β, and d_w.

GA, PS, and SA are performed in MATLAB R2019a, with Intel® $Core$™ i7-8700K, 3.7 GHz, x64 based processor, RAM-32 GB. Each optimization algorithm was run 10 times, and the best, average and worst values are recorded in Table 5. Values of these algorithms represent the maximum force applied by a coil to a magnetic shaft. The last row in this table is the average time each algorithm took to converge to a solution.

Table 5: The Best, Average, and worst Function value obtained using GA, SA, and PS. α, β, and d_w for best value are only written in the table.

	GA	SA	PS
Best Value, N/A	25.72	25.65	25.45
Average Value, N/A	25.59	25.26	25.45
Worst Value, N/A	25.45	23.93	25.45
Average Time, s	63.88	13.42	5.72
Coil Ratio α	1.45	1.37	1.48
Magnet Ratio β	1.52	1.51	1.80
Wire Diameter d_w	0.62	0.60	0.64

The function value for these algorithms was the maximum force of the coil applied to the magnet. Since the goal of this optimization was to maximize the force, it is shown from Table 5, GA obtained the highest force value in average, compare to SA and PS. It

is shown that PS found the same result every time. Even though GA took the longest to find the optimum, but it converged to the best optimum. The maximum normalized force achieved by GA was 25.72 N/A, and the optimum α, β, and d_w values were as follow.

$$\alpha = 1.45$$

$$\beta = 1.52$$

$$d_w = 0.62$$

The closest wire gauge to the optimum value is a 22 AWG wire, which is 0.64 mm in diameter.

Another series of optimizations were done using GA with the two variables α, and β as continuous variables and d_w as discrete variable. This optimization to find the maximum normalized force value was done for each wire gauge ranging from 12 AWG to 27 AWG. Figure 3.28 shows the comparison of normalized force with wire diameter. It is shown that 0.64 mm (22 AWG) corresponds to the maximum normalized force of 25.70 N/A with α = 1.47 and β =1.36. Please note that in this optimization, wire diameters were input as discrete numbers.

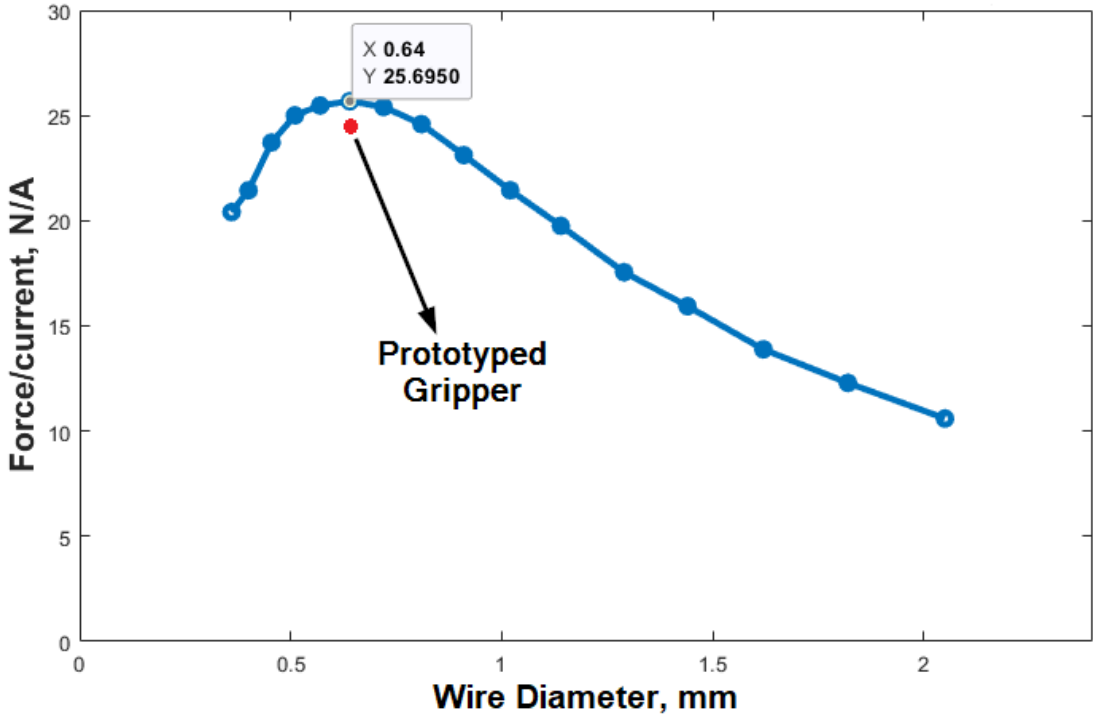

Figure 3.28: Optimized Normalized Force vs Coil's wire diameter

If we normalized the maximum force achieved by the prototyped gripper in Figure 3.25, the maximum experimental force of the prototyped would be 24.58 N/A using 0.64 mm copper wire. The red dot in Figure 3.28 compares the maximum normalized force achieved by the prototyped gripper with the optimization result. Therefore, the prototyped gripper can even be re-fabricated with the optimized design to even achieve a slightly higher maximum force.

3.3. Gripper Soft Membrane

The membrane in this gripper was one of the critical components to enhance the gripping strength. As mentioned earlier, the shaft was isolated from the main gripper's body and the flexible membrane was holding the shaft's weight when the coil was off. Therefore, this membrane needed to be strong enough to hold the weight of the shaft, but it also needed to be flexible enough to be able to form around the object being picked. Formation around the object being picked was due to positive pressure inside chamber when the shaft was being retracted. Researchers have used elastomeric polymers in robot for climbing smooth surfaces [90]–[93]. Adhesion of elastomeric pads better help these robots to climb a vertical surface.

In versions 1-4, I was using a party balloon as the membrane. A right size balloon was chosen and one cut was made at the stem and another cut on the other end. Then it was installed on the gripper as shown on Figure 3.4. Party balloon was made of Latex rubber and it was super thin. It was relatively strong but its stretch ability was limited and its surface friction was really low. It could never pick items that were damp.

In an effort to choose the best membrane for this gripper, different kinds of polymers were tested for flexibility, strength and friction. First few design prototypes were using commercially available pre-cured latex membrane or party balloons. Latex had a superior strength in compare to other polymers such as Silicone or polyurethane, but its stretch ability was really limited and it could not conform into smaller areas like the leaf on top of a fruit. Hence it could not create a good seal between the gripper and the object. Other polymers were created and investigated to choose the suitable one for this gripper. Table 6 shows specifications of the polymers that were investigated. Please note that EcoFlex™ 00-10 and Mold Max® 10t are Silicone rubbers, but VytaFlex™ 10 is a urethane rubber.

Table 6: Polymer Characteristics [94]

Polymer	Shore Hardness	Elongation at Break	100% Modulus
EcoFlex™ 00-10	00-10	800%	8 psi
VytaFlex™ 10	10 A	1000%	25 psi
Mold Max® 10t	10 A	526%	29 psi

EcoFlex™ 00-10 could stretch 800% of its size before it broke and it is about 200% less than VytaFlex™ 10. On the other hand, EcoFlex™ 00-10 needed a lot less force at 100% elongation which was considerably lower than VytaFlex™ 10. 100% modulus in Table 6 shows how much force is needed when a polymer is stretched 100%. Therefore, EcoFlex™ 00-10 was the membrane that was finally chosen for the gripper.

Shore hardness shown in Table 6 is the measure of hardness of a material. Shore 00 is for softer material and shore B is used for harder ones. In other words, shore hardness related directly to flexibility of the material and how easy it is to stretch. Figure 3.29 shows the shore hardness scale and the polymers mentioned in Table 6. EcoFlexTM 00-10 is on the soft side of this chart and its hardness is equal to marshmallow. Therefore,

EcoFlex™ 00-10 was much softer than the other two polymers and it could conform much easier on uneven surfaces.

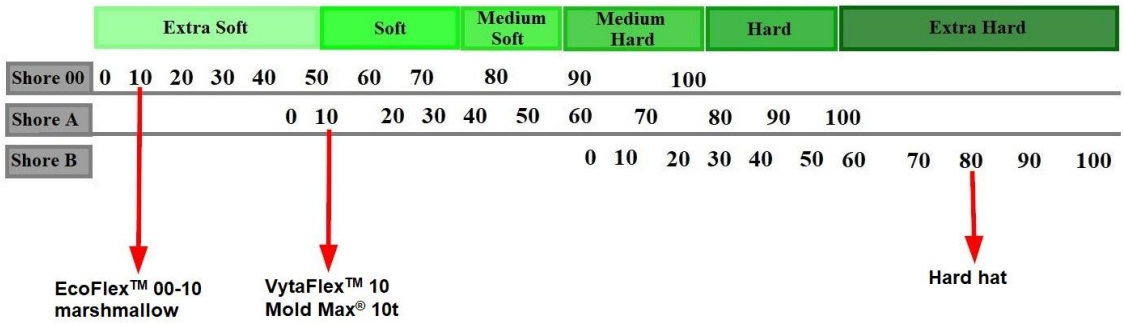

Figure 3.29: Shore Hardness scale (Modified from [95])

EcoFlex™ 00-10 was comparably much better than all the other polymers. It was much easier to stretch and conform into uneven surfaces. It could also hold a wet object or even objects with light soil around them due to its surface friction.

After choosing the right polymer, more research was done on the shape of this gripper's membrane and how it could be fabricated. An injection molding design was created using SolidWorks and it was printed in ABS plastic using a 3D printer. Figure 3.30 shows the designed mold for creating Silicone membrane using injection molding method. Silicone was injected using a syringe to four injection ports shown in Figure 3.30-a.

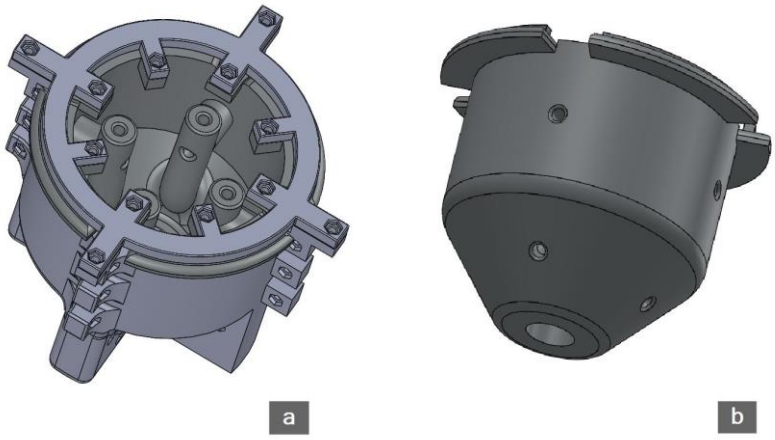

Figure 3.30: Injection molding prototype to create silicone membrane. a) Full assembled mold, b) Mold inner shell

Figure 3.31 shows the cured Silicone created using the designed mold. Unfortunately since the mold was 3D printed, it was porous. Imperfections could be seen all around the mold as it is shown in Figure 3.31-a, especially at lines were the outer shell pieces join together. In order to be able to separate the mold after silicone was cured, both shells of the mold were constructed from a few different pieces rather than just one outer shell and one inner shell.

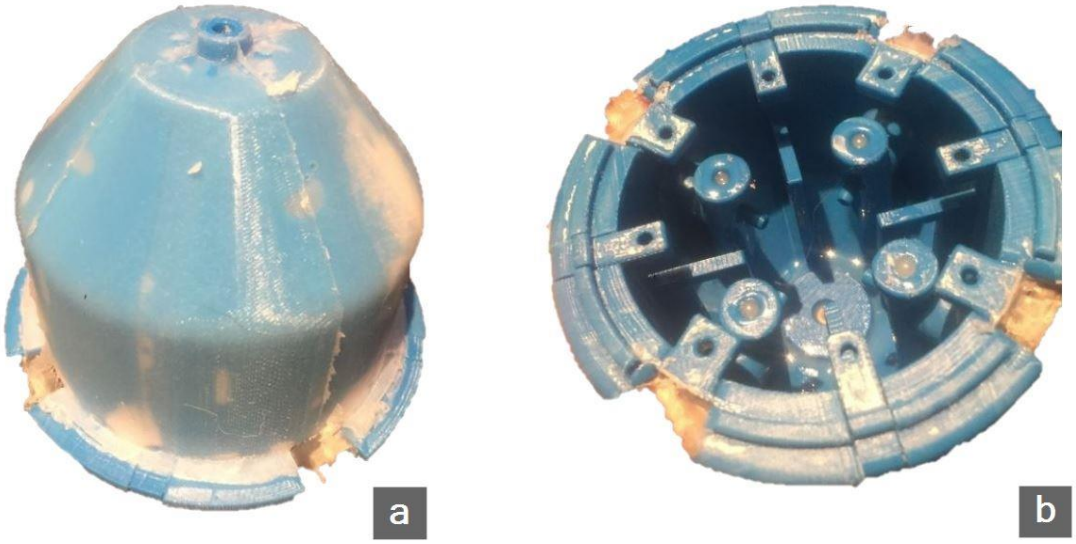

Figure 3.31: EcoFlex™ 00-10 created using an injection molding method

In order to have a perfect and accurate mold, Computer Numerical Control (CNC) machining was needed. Since these molds were just prototypes for testing, instead of creating molds using a CNC machine, Silicone was brushed on the cured membrane to get a better surface finish. Smoothness of the membrane's surface finish affects the friction between the object being picked and the membrane. Surface friction is much higher if we have a smooth surface finish on the gripper's membrane.

A few mold iterations in different shapes were created. Figure 3.32 shows these different molds, left column shows when the Silicone was being cured over the mold and right column shows when it was removed from the mold after it was cured. Silicone was applied using a brush over these molds. Due to the low viscosity of EcoFlex™ 00-10, it would flow down the mold and create a smooth surface when cured. Three to four layers of silicone had to be applied on these molds to get a desired thickness for the gripper's membrane.

Figure 3.32: Different Silicone mold iteration. Silicone was applied using a brush in these molds.

The mold used in Figure 3.32-a was the inner shell of the mold that was used for injection molding shown in Figure 3.30. But this time silicone was applied using a brush. As shown in Figure 3.32-a, the surface finish was not again as smooth as it was desired. Also the membrane bigger diameter was relatively big with respect to the gripper's chamber opening. It could fold when it was attached to the gripper and secured with the O-ring.

Then the mold shown in Figure 3.32-b was created and used. This mold was similar to the size and design of the party balloon that was being used before. In this mold a layer of silicone was applied and let dry placing the wine bottle on its bottom. Then another layer was applied and let dry placing the bottle upside down. This process was

done to have a more consistent thickness on the membrane, since silicone tends to flow down on the mold. This mold was much better than a party balloon made of Latex, but its connection to the shaft was not ideal since the shaft designed was changed from version 1-4. The membrane would have a lot of folds and wrinkles at the contact point with shaft.

Figure 3.32-c shows a wine bottle that is fixed to a jar using tape to have a stable stand. In this mold, the bottle end was covered using a Latex balloon to cover the imperfections at the bottom. Mold release was applied over the mold to ensure that silicone could easily be removed after it was cured. After the silicone was cured, a hole was made on the center of the flat side of the silicone. This side was connected to shaft as shown in Figure 3.10, and the other end was connected to the gripper's body as shown in Figure 3.9. This mold gave the best result in term of assembling on the gripper and shaft and also the performance. The reason wine bottle was chosen for these molds was that diameter ratio of the wine bottle to gripper's opening was about 75% and it allowed the membrane to be slightly stretched over the gripper body. Stretching the membrane eliminated wrinkles and folding of the membrane at contact points to the gripper's body. A big advantage of using the mold shown in Figure 3.32-c was the flat end of the mold. Since silicone could not flow down from this top to around the mold, it tended to be thicker on this end of the membrane when the mold was flat. When the gripper was picking an object, this part needed to be thicker due to the fact that it was stretched the most between the object and the shaft because of the shaft stroke.

A CAD model of a mold similar to the wine bottle was designed and 3D printed in ABS plastic. This mold also had a two-piece top cover to be try injecting Silicone again. The intention to use injection molding was to achieve a smooth finish and constant membrane thickness all around. But unfortunately, since the mold was 3D printed and not machined, it could not again achieve the requirements needed from and injection mold. Figure 3.33 shows this model. On the left, you can see the full mold with all its pieces, in the middle you only see the bottom piece of the mold, and the one on the right is the actual printed bottom piece of the mold with cured membrane covering it. As it is shown, the membrane had a lot of imperfections on the surface which were not ideal for our case. Also injection molding created more bubbles in the Silicone if the printed mold was not sealed and under vacuum.

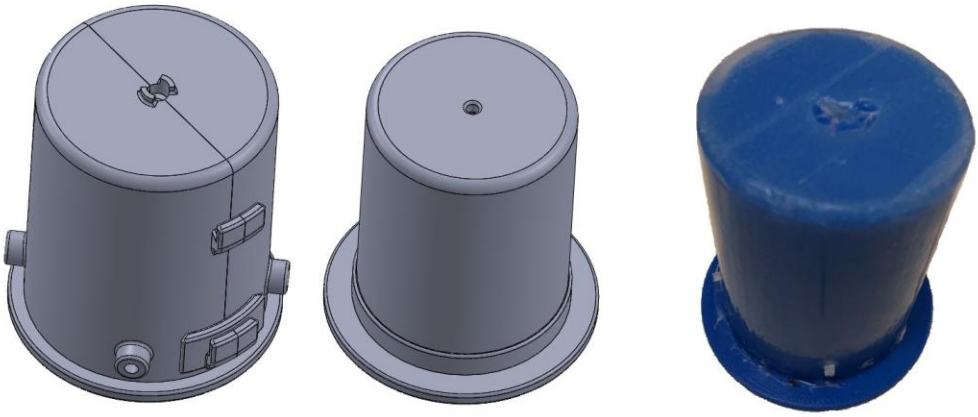

Figure 3.33: An injection mold Similar to the model of a wine bottle

At last a mold was derived from the wine bottle shape, but it was slightly modified to better improve the membrane for this gripper. As show in Figure 3.34 the top diameter was slightly reduced, and it merged to the bigger diameter with big diameter fillet. The reason for this modification was to reduce the wrinkles in membrane when it was being inflated. Since top part of the mold connects to the shaft, which is much smaller than the chamber, the mold diameter in this section needed to be about the same size as shaft's diameter but slightly bigger. This way, wrinkles in membrane were reduced when it was getting inflated.

Figure 3.34: Final Mold prototype

3.4. Gripper Electronics

As mentioned earlier, this gripper had a simple design and did not require complex control algorithms. An Arduino Uno microcontroller monitored and controlled all components of this gripper.

The controller for this prototype consisted of an Arduino controller, an air pressure sensor, a 2-channel relay module, and an infrared obstacle avoidance sensor module. Maximum voltage Arduino could supply was 5 V, but the coil needed over 5 V and the solenoid valve needed 12 V. Therefore, coil and solenoid valve were each connected to a channel of a mechanical relay module, where each channel was supplied with a separate power supply to provide the power needed for the coil and the solenoid valve. But Arduino controlled both relay channels. Infrared module and the pressure sensor were powered using Arduino's supplied voltage. Figure 3.35 shows the wiring diagram for the control box. The two power supplies used are adjustable. One power supply was set to 12V to supply both Arduino and Solenoid Valve, and the other power supply could be set based on the gripping strength needed for the coil. Please note that the Obstacle avoidance sensor in this drawing shows both the infrared sensor and the emitter attached to its board, but in the actual prototype the two LEDs were removed and attached to the gripper's chamber, connected to the obstacle avoidance sensor board using wires.

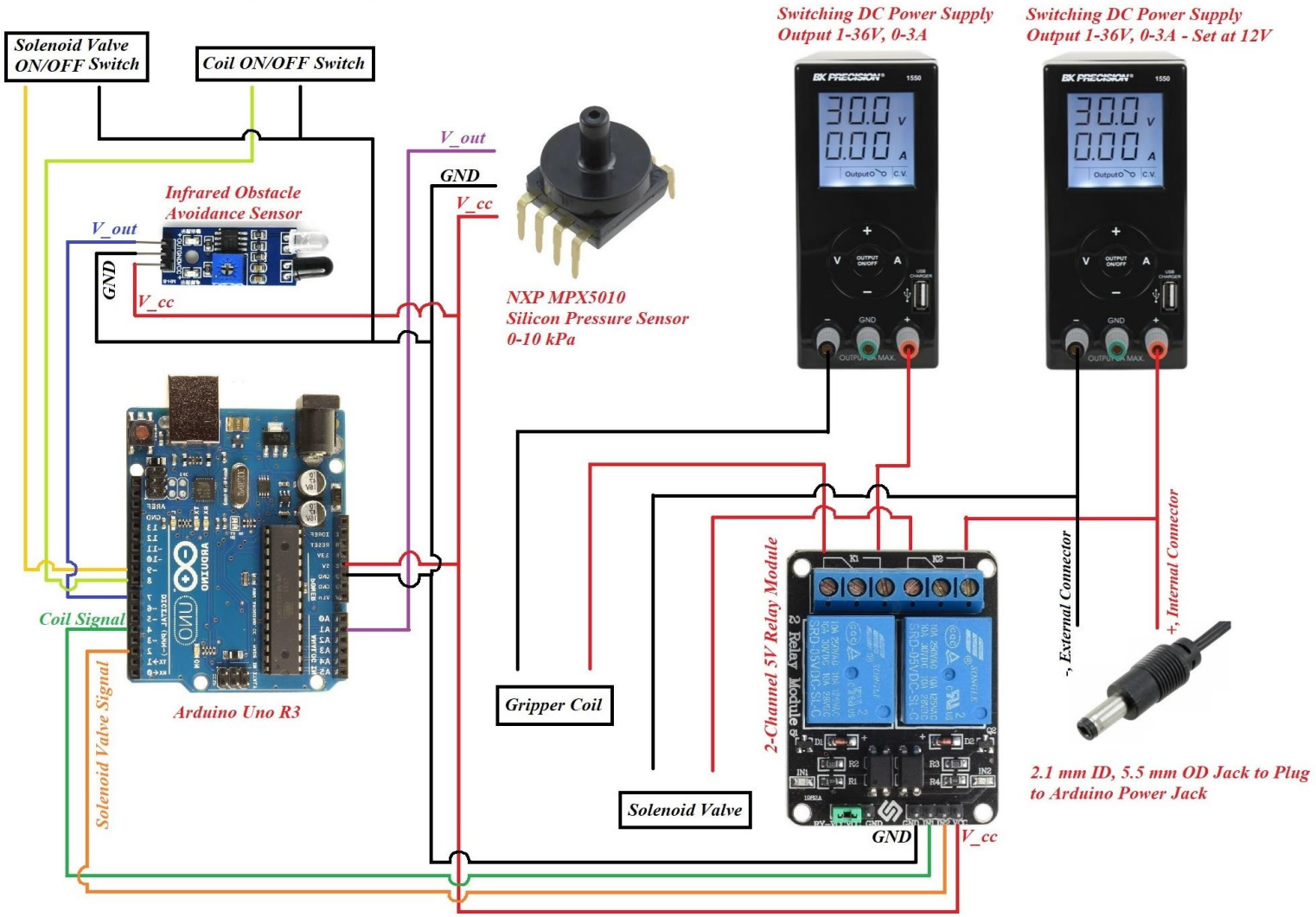

Figure 3.35: Control Box Wiring Diagram

Pressure sensor was not a critical component for operating the gripper, it only read pressure inside the sealed chamber and could be used to notify the controller if membrane seal was broken. As mentioned earlier, at the beginning of grasping process, shaft is pushed inside the gripper by movement of the KUKA arm, which is pushing the gripper over the object being picked. Infrared sensor senses the presence of shaft when it is almost in middle of chamber and triggers the coil to further move the shaft up. Once the grasped object is moved to the desired location, controller turns of the coil and opens the solenoid valve to get the pressure inside chamber to atmospheric pressure. The reason for opening the solenoid valve is that the prototype's main body was made of ABS plastic (even though air leakage was minimized), but we still have to neutralize the pressure inside chamber. Leakage was never reduced down to absolute zero. For the purpose of this tests, the coil and the solenoid valve activation and deactivation were done manually using two push button switches. The practical approach is to get real time feedback from KUKA's end effector and deactivate the coil or activate the solenoid valve respectively.

As mentioned earlier in this thesis the gripper could have a certain voltage and current applied to the coil based on coil's characteristics such as length, inner diameter, outer diameter, and wire gauge. In other words, the resistance that is created based the length and thickness of the wire used in the coil defines the relationship between voltage and current applied. If for certain requirement either a low voltage and high current coil, or a high voltage and low current coil is required, the coil can be wrapped in a combination of two or more coils in either series connection or parallel connection. In other words, if the coil's length and inner diameter are kept constant, the wire can be wrapped for about half the outer diameter size, and then another wire can be wrapped again around the same one until the desired outer diameter is reached. This way, the overall gripper's coil has four wire leads instead of two wire leads. So the finished two coil setup will look like a single coil, except that it consists of an inner coil with its own wire leads and an outer coil with its own wire leads. Then these four wire-leads for two coils can be connected either in series or parallel to meet the required specifications for voltage and current. An important factor to note here is the resistance of these two coils with respect to each other, and calculations should be done with respect to each coil before making the coil. For example, if the same wire gauge is used, the two coils are connected in parallel, and the inner coil has a smaller resistance than the outer coil, then the inner coil will have a higher current with respect to the outer coil.

The following example shows the difference between connecting two coils in series or parallel as explained above. Let us assume the inner coil has 4 Ω resistance and the outer coil has 6 Ω resistance, and a constant voltage of 10 V is applied. If we connect the two coils in series, the total coil current will be 1 A and each coil will also have 1 amp current. They basically act like we only wrapped a single wire. But if we connect the two coils in parallel, then the total coil current will be 4.17 A, the inner coil will have 2.5 A current and the outer coil will have 1.67 A current. Therefore, the inner coil has much higher current than outer coil applied.

Chapter 4.

Testing and Experiments

To address some parts of both objectives introduced in **Chapter 1**, this chapter presents four experiments conducted to evaluate the performance of the developed soft gripper in the context of common industrial tasks. **Section 4.1** investigates the peak power usage of the gripper, and **Section 4.2** analyses and illustrates the force loads of the gripper in a series of tasks involving picking up a spherical-shaped item. **Section 4.3** explores the gripper's actuation speed, and **Section 4.4**, evaluates the effectiveness of the gripper for real-world industrial applications by mounting it on a KUKA robotic arm, and conducting a diverse range of gripping tasks relevant to industrial contexts.

4.1. Peak power of the gripper

To better understand and analyse the power usage of the developed gripper, four stages were designed:

1) In Stage one, the gripper was put in idle, not holding any object. This stage serves as a baseline to analyse the minimum power consumption of the gripper, since the power consumption is solely from the controller board.

2) Stage two evaluates the peak power of the gripper with the coil turned on and set to its maximum power. In this stage, the shaft is pulled up the chamber with maximum achievable instant acceleration.

3) Stage three analyses the power usage of the gripper as it's is already gripping an object, and moving it to a predefined desired location. Since minimizing power was not our primary focus in this stage, we kept the coil constantly on for the gripper to move the object around. The power consumption during this stage can be significantly reduced by utilising a latching mechanism (to hold the shaft at the top), or reducing the coil power to just hold the object while moving it, as the coil's peak power is necessary only at the very first instant, when the shaft is pulled up to the top of gripper's chamber.

4) Stage four analyses the power consumption right after the gripper has released the object. In this stage, the gripper is not holding any object, but the actuated solenoid valve is opened to neutralize the pressure inside gripper's chamber to environment pressure. In stage four, the

gripper consumes the same power as in stage one, as well as the power consumed by the solenoid valve.

One of the most important advantages of this gripper is that it's gripping force and consequently its peak power usage can be adjusted depending on the object being picked. Since the main actuation force of the gripper is produced by a solenoid actuator (a coil and a magnetic shaft), we can always increase or decrease the current in the coil of the solenoid actuator to increase or decrease the resulting gripping force, respectively. Hence the peak power usage could be different depending on the current being applied. On the other hand, please note that power consumption in stage one and stage four were not adjustable since the usage is solely due to the controller and the solenoid actuated valve, however they were negligible.

Figure 4.1 shows the peak power in stages one, two, and four. Stage thee is not shown as it is analogous to stage two; In our prototype we just kept the coil to its peak power. Three different currents were applied to coil in stage two for comparison of peak power in different settings.

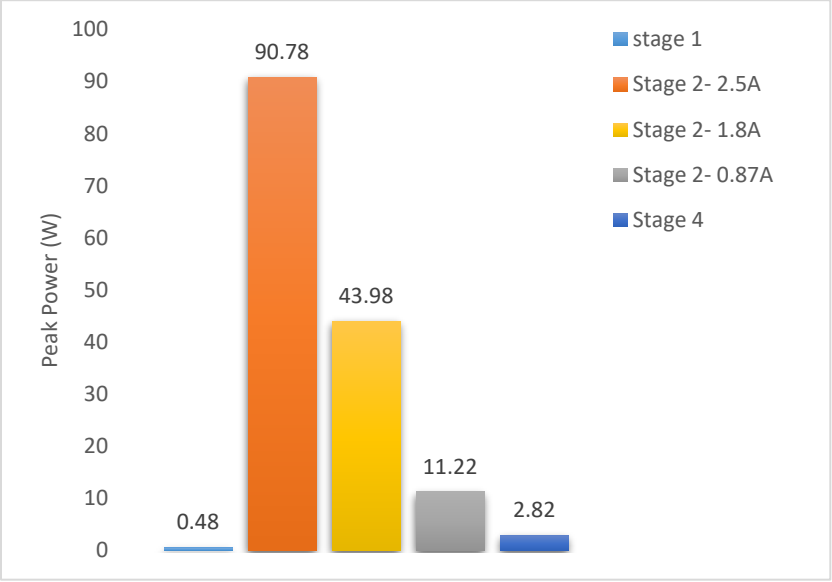

Figure 4.1: Peak Power of the gripper. Stages 1 and 4 peak powers are negligible, but stage 2 can be different depending on the current applied. 2.5 A, 1.8 A, and 0.87 A are shown.

4.2. Force Measurement

The goal of this section is to design a series of experiments to measure the maximum gripping force threshold of the designed gripper. To be relevant to industrial contexts, the gripper was mounted on a KUKA LBR iiwa robot [78].

The setup designed to measure the gripping force consisted of an ATI Industrial Automation Mini45 [96] sensor firmly fixed to a table using a 3D printed part, as well as an 89 mm diameter rubber ball fixed on top of the sensor visa a 3D printed adaptor. A well-rounded rubber ball was chosen to keep the measurements consistent and reliable. The setup is shown in Figure 4.2.

The experiment was designed such that initially the KUKA lowers the gripper towards the object until the gripper grasps the object, and the coil is activated. Next, the KUKA begins moving upwards causing the gripper to pull on the object in positive Z direction (towards the ceiling). The sensor measures the resulting force as the robot continues moving, until the grip is broken.

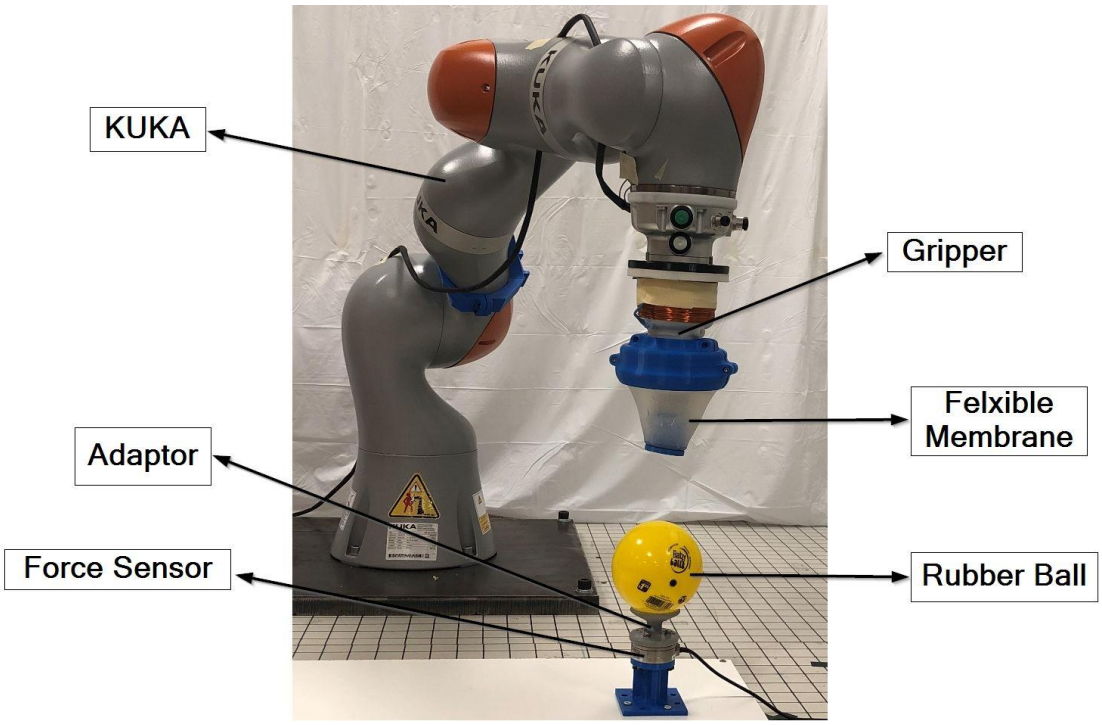

Figure 4.2: Force Measurement test setup

To measure the gripping force without suction, a through hole was made in the middle of the ball in order to eliminate the suction created by grippe. This hole was created on the top-center of the rubber ball and a tube was inserted through the ball. Figure 4.3 show the ball with a tube in center. Therefore, when the shaft was retracted by the coil, no suction could be formed between the shaft and the object. In this scenario, the normal force caused by the inflated membrane, as well as the friction force between the surface of the membrane and the object are the only driving forces holding the object.

Figure 4.3: A rubber ball with a tube inserted to create a hole

Figure 4.4 demonstrates how the applied current impacts the gripping force for three different currents (2.5 A, 1.8 A, and 0.87 A). The force was measured ten times for each current. The mean-peak force was then calculated for each current.

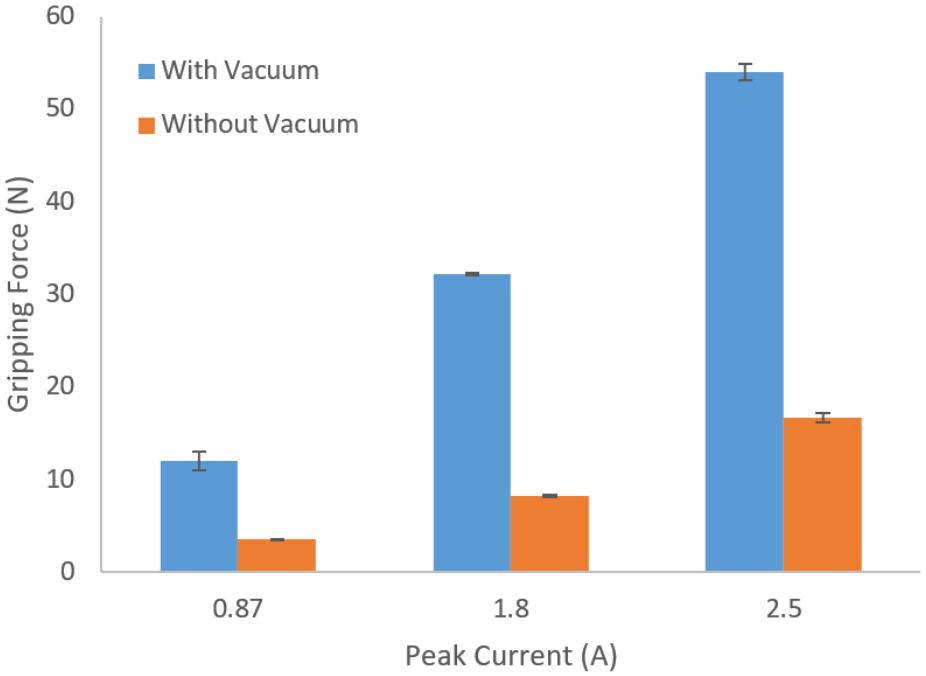

Figure 4.4: Force measurement results

The input power can be calculated from the set voltage, and the drawn current. Figure 4.5 shows how the gripping force changes according to the input power.

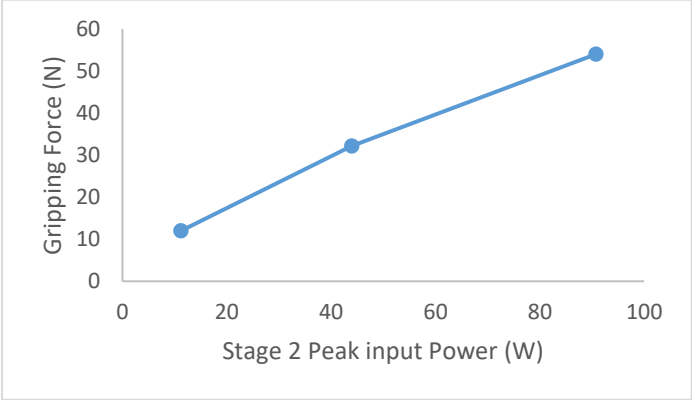

Figure 4.5: Gripping Force VS Gripper's input peak power

4.3. Actuation Speed

One of the biggest advantages of the magnetic gripper is the use of a coil as an actuator. The gripper's magnetic shaft and the coil work as a solenoid for actuating the shaft and gripping objects, enabling very high actuation speeds. When 2.5 A current was supplied to the coil, the corresponding actuation speed was measured at 0.88 m/s. Figure 4.6 shows how the actuation speed of the gripper changes with the input power. To be consistent with our previous analysis (Section 4.2), the actuation speed is shown as a function of the peak power of the gripper. The higher the input power, the higher the actuation speed would be. Shaft movement of the gripper was recorded using an Iphone X camera at 240 frames per second, and shaft's speed was calculated based on the traveled distance over each time segment.

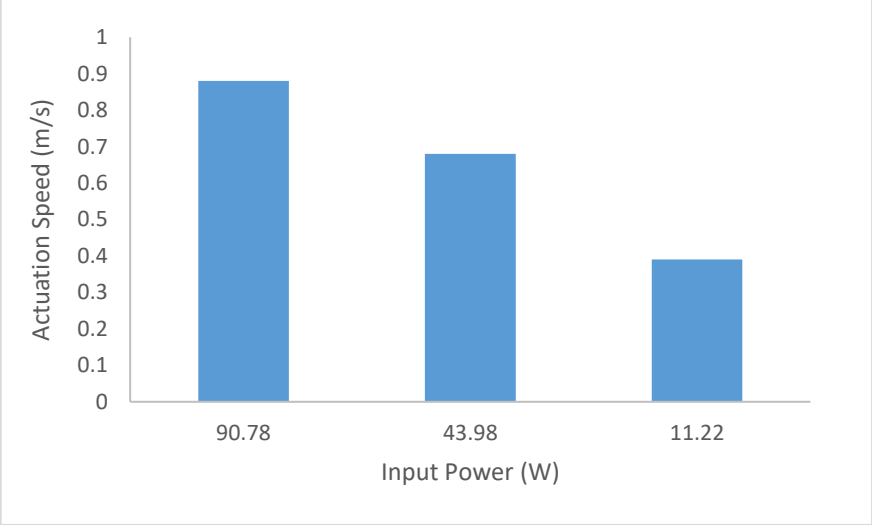

Figure 4.6: Gripper actuation speed vs input power

4.4. Picking up Objects with Different Shapes and Weights

The gripper was tested with various known objects to check its ability to pick up different objects with varying shapes and weights. Figure 4.7 shows an example set of objects picked up by the gripper in a series tests using a KUKA arm. Due to its simple design and mechanism, the gripper has the potential to be rescaled according to the task at hand to be able to grip a wide variety of objects in size, geometry, and texture.

As shown in Figure 4.7, the developed prototype here can still pick up wide range of objects without requiring rescaling. This includes objects with different surface finishes

like a flat smooth surface (Figure 4.7-D), a relatively rough surface (Figure 4.7-O), light and delicate objects (Figure 4.7-A and Figure 4.7-H), as well as much heavier ones.

Some examples of these objects include an apple in different orientations (Figure 4.7-A, and Figure 4.7-B), a 796 mL tomato paste steel can (Figure 4.7-C), an acrylic display riser with a flat smooth surface (Figure 4.7-D), a box of Coke soda cans weighting about 2.95 Kg measuring 23 cm x 14 cm x 12 cm (8 cans of 355 mL, Figure 4.7-E), a 2 L Pepsi bottle (Figure 4.7-F), a honey dew about 2.5 Kg (Figure 4.7-G), a light bulb (Figure 4.7-H), a 591 mL VitaminWater in different orientations (Figure 4.7-I, and Figure 4.7-J), a 355 mL Red Bull energy drink in different orientations (Figure 4.7-K, and Figure 4.7-L), a tomato in different orientations (Figure 4.7-M, and Figure 4.7-N), a football with a rough surface (Figure 4.7-O), a 0.74 Kg mixed nut container (Figure 4.7-P), a watermelon (Figure 4.7-Q), a ream of letter size paper (Figure 4.7-R), and an oversized drone box about 1.9 Kg and measuring 58 cm x 57 cm x 14 cm (Figure 4.7-S).

Figure 4.7: Picking up objects with various shapes and weights.

Figure 4.8 shows more complicated gripping scenarios. First and third columns of Figure 4.8 show the objects from the perspective of the gripper, where it is supposed to be in contact with gripper's membrane.

Figure 4.8-A shows a bell pepper from the side where it has the most unevenness in shape. Figure 4.8-B is a grapefruit which has a porous surface and can be slightly damp due to the fruit's nature. Figure 4.8-C is a lime which has similar surface to the grapefruit. Figure 4.8-D is a bag of 66 g chips. Figure 4.8-E is a pair of jeans wrapped manually in a really thin nylon, showing how the gripper can lift this by just grabbing the loose nylon. Figure 4.8-F is a tennis ball which is porous, showing the gripping action without any suction. Figure 4.8-G is an empty box that is relatively large, showing how the gripper can pick even when it is not picking an item from the center point. Figure 4.8-H is a full fire extinguisher that is about 3.5 kg.

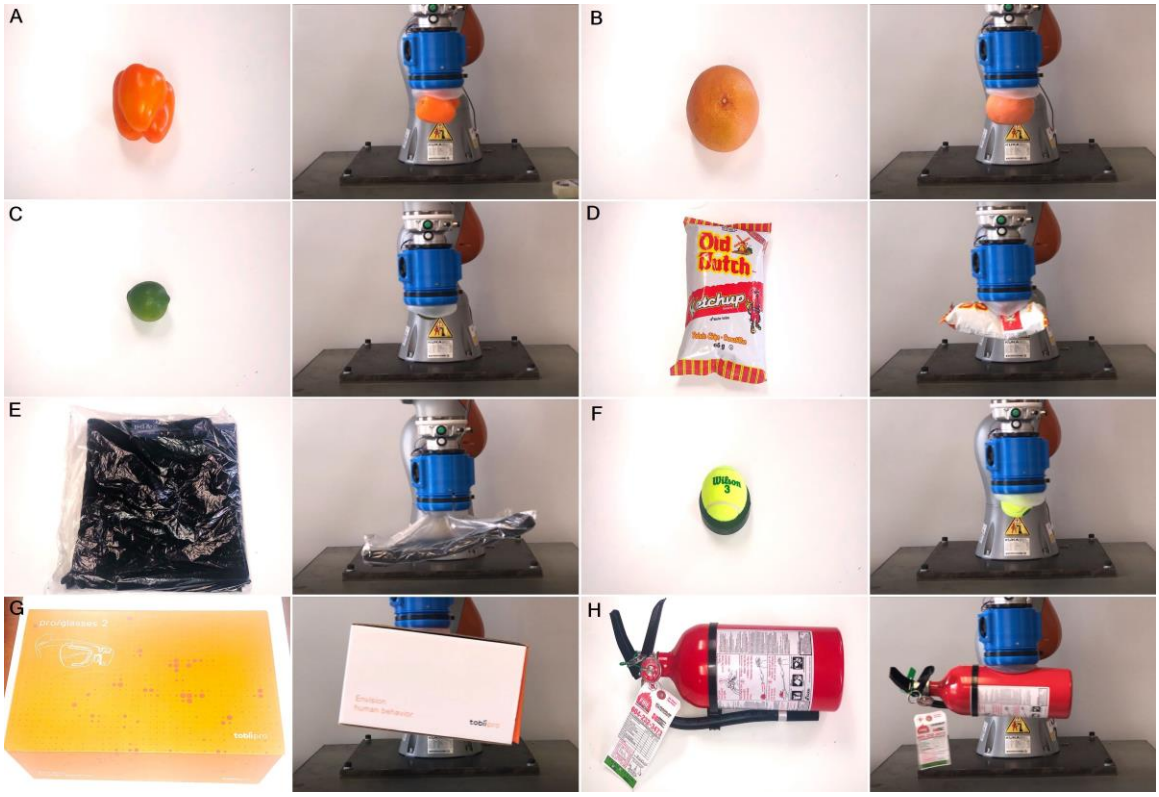

Figure 4.8: Gripping various objects and a picture of their contact point with the gripper

Chapter 5.

Conclusion

This chapter summarizes the thesis work and reviews the key contributions of this work.

Objective 1: The first objective of this work was the design and fabrication of a novel robotic gripper that could be implemented in a wide range of industrial applications. A micro-controller drives the gripper, allowing for a simple control mechanism of the gripper both in hardware and software. The gripper's body is fixed to a robotic arm's end effector and the shaft assembly is the only movable part in the design of this gripper, hence mechanical wear and tear of the gripper is minimal.

The gripper's final dimensions are 11.5 cm in diameter and 15.5 cm in length (1582 cm^2) when the shaft is fully extended (considering the maximum volume it can occupy as a solid cylinder in space). This confirms that the gripper is compact and has about the same dimensions compared to other commercially available grippers for collaborative robots.

The gripper's chamber is sealed using a silicone soft membrane. This membrane is the contact point of the gripper with the object being picked allowing grasping of objects with different shapes and even very delicate objects like fruits or a light bulb possible without any excessive pressure that could damage the object. Another advantage of the silicone membrane is that it can conform to the surface of the object at its contact point. As the gripper gets closer to the object, the membrane inflates around the object, allowing gripping of the target object without the need for accurate alignment of the end effector with the object's orientation.

Unlike most robotic grippers such as anthropomorphic grippers or the ones with suction cups, the proposed gripper can pick target objects from clustered environments. The soft membrane can come in contact with the target surface from most orientations and still form strong suction.

Objective 2: To address the second objective of this work an actuator was designed for this gripper without requiring any additional equipment (e.g. pressure air line) for functionality making it a self-contained gripper.

The gripper's actuation mechanism consists of a solenoid actuator with a magnetic shaft, allowing for fast gripping action. The mean actuation speed of the gripper was measured at 0.88 m/s, which is much higher than 0.2 m/s proposed in the objective. In addition, the magnetic shaft increases the solenoid actuator's force and makes the shaft bidirectional in contrast to other solenoid actuators with an iron shaft.

Another advantage of this gripper is that peak power can be adjusted depending on intended objects being picked. The griping force consists of friction forces due to the normal force between the surface of the silicone membrane and the object, as well as the suction force of the gripper.

To test and evaluate the effectiveness of the designed gripper in relevant industrial applications, a series of pick-and-place experiments were conducted with the gripper mounted on a KUKA robotic arm. The gripper was successfully tested on a variety of everyday objects from simple ones such fruits, snacks, clothing, and health essentials to more complicated objects like a heavy fire extinguisher about 3.5 Kg, a cloth in a very loose plastic bag, and an oversized box (Section 4.4).

References

[1] C. Ray, F. Mondada, and R. Siegwart, “What do people expect from robots?,” in *2008 IEEE/RSJ International Conference on Intelligent Robots and Systems*, 2008, pp. 3816–3821.

[2] R. Pfeifer and M. Lungarella, “The Challenges Ahead for Bio-Inspired ‘Soft’ Robotics,” *Commun. ACM*, vol. 55, no. 11, pp. 76–87, 2012.

[3] B. Matthias, S. Kock, H. Jerregard, M. Kallman, and I. Lundberg, “Safety of collaborative industrial robots: Certification possibilities for a collaborative assembly robot concept,” in *IEEE International Symposium on Assembly and Manufacturing*, 2011, pp. 1–6.

[4] J. Kruger, T. K. Lien, and A. Verl, “Cooperation of human and machines in assembly lines,” *CIRP Ann.*, vol. 58, no. 2, pp. 628–646, Jan. 2009.

[5] G. J. Monkman, S. Hesse, R. Steinmann, and H. Schunk, *Robot grippers*. Germany: John Wiley & Sons: Weinheim, 2007.

[6] A. Bertelsen, J. Melo, E. Sánchez, and D. Borro, “A review of surgical robots for spinal interventions,” *Int. J. Med. Robot. Comput. Assist. Surg.*, vol. 9, no. 4, pp. 407–422, Dec. 2013.

[7] K. Tai *et al.*, “State of the Art Robotic Grippers and Applications,” *Robotics*, vol. 5, no. 2, p. 11, Jun. 2016.

[8] A. Pattersson, T. Ohlsson, S. Davis, J. O. Gray, and T. J. Dodd, “A hygienically designed force gripper for flexible handling of variable and easily damaged natural food products,” *Innov. Food Sci. Emerg. Technol.*, vol. 12, no. 3, pp. 344–351, Jul. 2011.

[9] G. Fantoni *et al.*, “Grasping devices and methods in automated production processes,” *CIRP Ann.*, vol. 63, no. 2, pp. 679–701, Jan. 2014.

[10] F. Biganzoli and G. Fantonib, “A self-centering electrostatic microgripper,” *J. Manuf. Syst.*, vol. 27, no. 3, pp. 136–144, Jul. 2008.

[11] S. Tiefeng, D. Mingyu, B. Guanjun, Z. Libin, and Y. Qinghua, “Fruit harvesting continuum manipulator inspired by elephant trunk,” *Int. J. Agric. Biol. Eng.*, vol. 8, no. 1, pp. 57–63, Feb. 2015.

[12] K. Sangbae, C. Laschi, and B. Trimmer, “Soft robotics: a bioinspired evolution in robotics,” *Trends Biotechnol.*, vol. 31, no. 5, pp. 287–294, May 2013.

[13] J. Amend, E. Brown, N. Rodenberg, H. Jaeger, and H. Lispn, “A positive pressure

universal gripper based on the jamming of granular material," *IEEE Trans. Robot.*, vol. 28, no. 2, pp. 341–350, 2012.

[14] N. G. Cheng *et al.*, "Design and Analysis of a Robust, Low-cost, Highly Articulated manipulator enabled by jamming of granular media," in *2012 IEEE International Conference on Robotics and Automation*, 2012, pp. 4328–4333.

[15] C. Laschi, M. Cianchetti, B. Mazzolai, L. Margheri, M. Follador, and P. Dario, "Soft Robot Arm Inspired by the Octopus," *Adv. Robot.*, vol. 26, no. 7, pp. 709–727, Jan. 2012.

[16] "Products | OnRobot." [Online]. Available: https://onrobot.com/en/products. [Accessed: 10-Dec-2019].

[17] H. D. Bos and I. Wassink, "Evolution of Robotic Hands," *Univ. Twente*, 2010.

[18] D. Alba, M. Armada, and R. Ponticelli, "An Introductory Revision to Humanoid Robot Hands," in *Climbing and Walking Robots*, Berlin, Heidelberg: Springer Berlin Heidelberg, 2005, pp. 701–712.

[19] J. Krahn, F. Fabbro, and C. Menon, "A soft-touch gripper for grasping delicate objects," *IEEE/ASME Trans. Mechatronics*, vol. 22, no. 3, pp. 1276–1286, 2017.

[20] M. Grebenstein, M. Chalon, and W. Friedl, "The hand of the DLR hand arm system: Designed for interaction," *Int. J. Rob. Res.*, vol. 31, no. 13, pp. 1531–1555, 2012.

[21] M. A. Roa and R. Suárez, "Grasp quality measures: review and performance," *Auton. Robots*, vol. 38, no. 1, pp. 65–88, Jan. 2015.

[22] R. Boughdiri, H. Nasser, H. Bezine, N. Sirdi, A. Alimi, and A. Naakmane, "Dynamic modeling and control of a multi-fingered robot hand for grasping task," *Procedia Eng.*, vol. 41, pp. 923–931, 2012.

[23] J. Kerr and B. Roth, "Analysis of Multifingered Hands," *Int. J. Rob. Res.*, vol. 4, no. 4, pp. 3–17, Jan. 1986.

[24] H. Choi and M. Koc, "Design and feasibility tests of a flexible gripper based on inflatable rubber pockets," *Int. J. Mach. Tools Manuf.*, vol. 46, no. 12–13, pp. 1350–1361, 2006.

[25] T. Laliberté, L. Birglen, and C. M. Gosselin, "Underactuation in robotic grasping hands," 2002.

[26] S. Montambault and C. M. Gosselin, "Analysis of underactuated mechanical grippers," *J. Mech. Des. Trans. ASME*, vol. 123, no. 3, pp. 367–374, 2001.

[27] J. D. Crisman, C. Kanojia, and I. Zeid, "Graspar: A flexible, easily controllable

robotic hand," *IEEE Robot. Autom. Mag.*, vol. 3, no. 2, pp. 32–38, Jun. 1996.

[28] R. M. Crowder and D. R. Whatley, "Robotic gripping device having linkage actuated finger sections," US4834443A, 1986.

[29] S. J. Bartholet, "Reconfigurable end effector," US5108140A, 1990.

[30] T. Nishimura, K. Mizushima, Y. Suzuki, T. Tsuji, and T. Watanabe, "Variable-Grasping-Mode Underactuated Soft Gripper with Environmental Contact-Based Operation," *IEEE Robot. Autom. Lett.*, vol. 2, no. 2, pp. 1164–1171, Apr. 2017.

[31] L. U. Odhner *et al.*, "A compliant, underactuated hand for robust manipulation," *Int. J. Rob. Res.*, vol. 33, no. 5, pp. 736–752, Apr. 2014.

[32] F. Ilievski, A. D. Mazzeo, R. F. Shepherd, X. Chen, and G. M. Whitesides, "Soft robotics for chemists," *Angew. Chemie - Int. Ed.*, vol. 50, no. 8, pp. 1890–1895, 2011.

[33] R. Deimel and O. Brock, "A compliant hand based on a novel pneumatic actuator," *IEEE Int. Conf. Robot. Autom.*, 2013.

[34] M. E. Giannaccini *et al.*, "A variable compliance, soft gripper," *Auton. Robots*, vol. 36, no. 1–2, pp. 93–107, Jan. 2014.

[35] R. Kolluru, K. P. Valavanis, and T. M. Hebert, "Modeling, analysis, and performance evaluation of a robotic gripper system for limp material handling," *IEEE Trans. Syst.*, vol. 28, no. 3, pp. 480–486, 1998.

[36] R. Kolluru, K. P. Valavanis, S. S. Smith, and N. Tsourveloudis, "Design fundamentals of a reconfigurable robotic gripper system," *IEEE Trans. Syst.*, vol. 30, no. 2, pp. 181–187, 200AD.

[37] J. Shintake, V. Cacucciolo, D. Floreano, and H. Shea, "Soft Robotic Grippers," *Adv. Mater.*, vol. 30, no. 29, pp. 1–33, 2018.

[38] E. Brown *et al.*, "Universal robotic gripper based on the jamming of granular material," *Proc. Natl. Acad. Sci.*, vol. 107, no. 44, pp. 18809–18814, Nov. 2010.

[39] W. Zesch, M. Brunner, and A. Weber, "Vacuum tool for handling microobjects with a NanoRobot," *Proc. Int. Conf. Robot. Autom.*, no. April, pp. 1761–1766, 1997.

[40] F. Maghooa, A. Stilli, Y. Noh, K. Althoefer, and H. A. Wurdemann, "Tendon and pressure actuation for a bio-inspired manipulator based on an antagonistic principle," in *Proceedings - IEEE International Conference on Robotics and Automation*, 2015, vol. 2015-June, no. June, pp. 2556–2561.

[41] A. Pettersson, S. Davis, J. O. Gray, T. J. Dodd, and T. Ohlsson, "Design of a magnetorheological robot gripper for handling of delicate food products with

varying shapes," *J. Food Eng.*, vol. 98, no. 3, pp. 332–338, Jun. 2010.

[42] F. Erzincanli and J. M. Sharp, "Meeting the need for robotic handling of food products," *Food Control*, vol. 8, no. 4, pp. 185–190, 1997.

[43] S. Davis, J. O. Gray, and D. G. Caldwell, "An end effector based on the Bernoulli principle for handling sliced fruit and vegetables," *Robot. Comput. Integr. Manuf.*, vol. 24, no. 2, pp. 249–257, Apr. 2008.

[44] A. Pettersson, T. Ohlsson, S. Davis, J. O. Gray, and T. J. Dodd, "A hygienically designed force gripper for flexible handling of variable and easily damaged natural food products," *Innov. Food Sci. Emerg. Technol.*, vol. 12, no. 3, pp. 344–351, Jul. 2011.

[45] Z. Wang, Y. Torigoe, and S. Hirai, "A Prestressed Soft Gripper: Design, Modeling, Fabrication, and Tests for Food Handling," *IEEE Robot. Autom. Lett.*, vol. 2, no. 4, pp. 1909–1916, Oct. 2017.

[46] T. Tarvainen and W. Yu, "Pneumatic Multi-Pocket Elastomer Actuators for Metacarpophalangeal Joint Flexion and Abduction-Adduction," *Actuators*, vol. 6, no. 3, p. 27, 2017.

[47] K. Suzumori, S. Iikura, and H. Tanaka, "Development of flexible microactuator and its applications to robotic mechanisms," *IEEE Int. Conf. Robot. Autom.*, 1991.

[48] K. Suzumori, S. Iikura, and H. Tanaka, "Applying a flexible microactuator to robotic mechanisms," *IEEE Control Syst. Mag.*, vol. 12, no. 1, p. 21.27, 1992.

[49] S. Terryn, J. Brancart, D. Lefeber, G. Van Assche, and B. Vanderborght, "Self-healing soft pneumatic robots," *Sci. Robot.*, vol. 2, no. 9, p. eaan4268, 2017.

[50] N. America *et al.*, "High-Speed Electrically Actuated Elastomers with Strain Greater Than 100 %," vol. 287, no. February, pp. 836–840, 2000.

[51] S. Song, C. Majidi, and M. Sitti, "GeckoGripper: A soft, inflatable robotic gripper using gecko-inspired elastomer micro-fiber adhesives," *IEEE Int. Conf. Intell. Robot. Syst.*, no. Iros, pp. 4624–4629, 2014.

[52] G. Monkman, "Electroadhesive microgrippers," *Ind. Rob.*, vol. 30, no. 4, pp. 326–330, 2003.

[53] J. Shintake, S. Rosset, B. Schubert, D. Floreano, and H. Shea, "Versatile Soft Grippers with Intrinsic Electroadhesion Based on Multifunctional Polymer Actuators," *Adv. Mater.*, vol. 28, no. 2, pp. 231–238, 2016.

[54] E. W. Schaler, D. Ruffatto, P. Glick, V. White, and A. Parness, "An electrostatic gripper for flexible objects," *IEEE Int. Conf. Intell. Robot. Syst.*, vol. 2017-Septe,

pp. 1172–1179, 2017.

[55] M. Calisti *et al.*, “An octopus-bioinspired solution to movement and manipulation for soft robots,” *Bioinspiration and Biomimetics*, vol. 6, no. 3, 2011.

[56] D. Rus and M. T. Tolley, “Design, fabrication and control of soft robots,” *Nature research journal*, vol. 521, no. 7553. Nature Publishing Group, pp. 467–475, 27-May-2015.

[57] M. Manti, T. Hassan, G. Passetti, N. D’Elia, M. Cianchetti, and C. Laschi, “An under-actuated and adaptable soft robotic gripper,” in *Biomimetic and Biohybrid Systems. Living Machines 2015*, 2015, vol. 9222, pp. 64–74.

[58] R. Bogue, “Flexible and soft robotic grippers: The key to new markets?,” *Ind. Rob.*, vol. 43, no. 3, pp. 258–263, May 2016.

[59] “Soft Robotics.” [Online]. Available: https://www.softroboticsinc.com/. [Accessed: 05-Dec-2019].

[60] “FlexShapeGripper | Festo Corporate.” [Online]. Available: https://www.festo.com/group/en/cms/10217.htm. [Accessed: 05-Dec-2019].

[61] “Suction cups, Vacuum cups, Vacuum pads.” [Online]. Available: http://www.vacmotion.com/Suction Cups.htm. [Accessed: 20-Jun-2019].

[62] D. Rus and M. T. Tolley, “Design, fabrication and control of soft robots,” *Nature*, vol. 521, no. 7553, pp. 467–475, May 2015.

[63] B. H. Shin, K. M. Lee, and S. Y. Lee, “A Miniaturized Tadpole Robot Using an Electromagnetic Oscillatory Actuator,” *J. Bionic Eng.*, vol. 12, no. 1, pp. 29–36, 2015.

[64] D. Ebihara and M. Watada, “Development of A Single-winding Linear Oscillatory Actuator,” *IEEE Trans. Magn.*, vol. 28, no. 5, pp. 3030–3032, 1992.

[65] B. Lequesne, “Fast-Acting Long-Stroke Bistable Solenoids with Moving Permanent Magnets,” *IEEE Trans. Ind. Appl.*, vol. 26, no. 3, pp. 401–407, 1990.

[66] N. Borcea, A. D. Ionescu, and M. S. Barbulescu, “Electromagnetic gripper assembly,” US4667998A, 1987.

[67] S. R. Covert, J. P. Moore, and J. M. Rhoades, “Tube gripper device,” US5775755A, 1997.

[68] J. W. Geary and P. E. McCormic, “Solenoid gripper,” US8186733B2, 2012.

[69] J. Kim and J. Chang, “A new electromagnetic linear actuator for quick latching,” in *IEEE Transactions on Magnetics*, 2007, vol. 43, no. 4, pp. 1849–1852.

[70] R. B. Van Varseveld and G. M. Bone, “Accurate position control of a pneumatic

actuator using on/off solenoid valves," *IEEE/ASME Trans. Mechatronics*, vol. 2, no. 3, pp. 195–204, 1997.

[71] C. Song and S. Lee, "Design of a solenoid actuator with a magnetic plunger for miniaturized segment robots," *Appl. Sci. J.*, vol. 5, no. 3, pp. 595–607, 2015.

[72] S. Bammesberger *et al.*, "A Low-Cost, Normally Closed, Solenoid Valve for Non-Contact Dispensing in the Sub-µL Range," *Micromachines*, vol. 4, no. 1, pp. 9–21, Feb. 2013.

[73] S. Kartmann, P. Koltay, R. Zengerle, and A. Ernst, "A Disposable Dispensing Valve for Non-Contact Microliter Applications in a 96-Well Plate Format," *Micromachines*, vol. 6, no. 4, pp. 423–436, Apr. 2015.

[74] "Standard Stock Coils | Electromagnetic Solenoid Coils | APW Company." [Online]. Available: https://apwelectromagnets.com/standard-coils/. [Accessed: 05-Jun-2018].

[75] "Industrial Robot Finder Tool | FANUC America." [Online]. Available: https://www.fanucamerica.com/products/robots/robot-finder-tool. [Accessed: 03-Jun-2018].

[76] "Silicone Rubber - Platinum Cure from Smooth-On, Inc." [Online]. Available: https://www.smooth-on.com/category/platinum-silicone/. [Accessed: 10-Jul-2019].

[77] "High Temp Resin 1 L | Formlabs." [Online]. Available: https://formlabs.com/store/form-2/materials/high-temp-resin/. [Accessed: 01-Aug-2019].

[78] "LBR iiwa | KUKA AG." [Online]. Available: https://www.kuka.com/en-ca/products/robotics-systems/industrial-robots/lbr-iiwa. [Accessed: 17-Jun-2019].

[79] "American Wire Gauge Chart and AWG Electrical Current Load Limits table with ampacities, wire sizes, skin depth frequencies and wire breaking strength." [Online]. Available: https://www.powerstream.com/Wire_Size.htm. [Accessed: 26-Jun-2019].

[80] W. Robertson, B. Cazzolato, and A. Zander, "Axial force between a thick coil and a cylindrical permanent magnet: Optimizing the geometry of an electromagnetic actuator," *IEEE Trans. Magn.*, vol. 48, no. 9, pp. 2479–2487, 2012.

[81] W. Robertson, B. Cazzolato, and A. Zander, "A simplified force equation for coaxial cylindrical magnets and thin coils," *IEEE Trans. Magn.*, vol. 47, no. 8, pp. 2045–2049, 2011.

[82] "MAGCODE: models for calculating magnetic fields and interactions_GitHub."

[Online]. Available: https://github.com/wspr/magcode. [Accessed: 23-Jan-2019].

[83] H. M. Pandey, A. Chaudhary, and D. Mehrotra, “A comparative review of approaches to prevent premature convergence in GA,” *Applied Soft Computing Journal*, vol. 24. Elsevier Ltd, pp. 1047–1077, 2014.

[84] H. M. Pandey, M. Rajput, and V. Mishra, “Performance comparison of pattern search, simulated annealing, genetic algorithm and jaya algorithm,” in *Advances in Intelligent Systems and Computing*, 2018, vol. 542, pp. 377–384.

[85] B. Ozpineci, L. M. Tolbert, and J. N. Chiasson, “Harmonic optimization of multilevel converters using genetic algorithms,” in *PESC Record - IEEE Annual Power Electronics Specialists Conference*, 2004, vol. 5, pp. 3911–3916.

[86] A. Dekkers and E. Aarts, “Global optimization and simulated annealing,” *Math. Program.*, vol. 50, no. 1–3, pp. 367–393, Mar. 1991.

[87] S. A. Kravitz and R. A. Rutenbar, “Placement by Simulated Annealing on a Multiprocessor,” *IEEE Trans. Comput. Des. Integr. Circuits Syst.*, vol. 6, no. 4, pp. 534–549, 1987.

[88] V. Torczon, “Pattern Search Methods for Nonlinear Optimization,” 1995.

[89] J. W. Chinneck, *PRACTICAL OPTIMIZATION: A GENTLE INTRODUCTION*. 2015.

[90] K. A. Daltorio, S. Gorb, A. Peressadko, A. D. Horchler, R. E. Ritzmann, and R. D. Quinn, “A Robot that Climbs Walls using Micro-structured Polymer Feet,” in *Climbing and Walking Robots*, Berlin, Heidelberg: Springer Berlin Heidelberg, 2006, pp. 131–138.

[91] O. Unver, “Geckobot : A Gecko Inspired Climbing Robot Using Elastomer Adhesives,” no. May, pp. 2329–2335, 2006.

[92] D. Santos, S. Kim, M. Spenko, A. Parness, and M. Cutkosky, “Directional adhesive structures for controlled climbing on smooth vertical surfaces,” *Proc. - IEEE Int. Conf. Robot. Autom.*, no. April, pp. 1262–1267, 2007.

[93] D. Santos, B. Heyneman, S. Kim, N. Esparza, and M. R. Cutkosky, “Gecko-inspired climbing behaviors on vertical and overhanging surfaces,” *Proc. - IEEE Int. Conf. Robot. Autom.*, pp. 1125–1131, 2008.

[94] “Smooth-On Materials Documents.” [Online]. Available: https://www.smooth-on.com/documents/. [Accessed: 05-Jun-2018].

[95] “Durometer Shore Hardness Scale.” [Online]. Available: https://www.smooth-on.com/page/durometer-shore-hardness-scale/. [Accessed: 09-Sep-2018].

[96] “ATI Industrial Automation: F/T Sensor Mini45.” [Online]. Available: https://www.ati-ia.com/products/ft/ft_models.aspx?id=Mini45. [Accessed: 06-Aug-2019].